TECHNICAL NOTE N° IDB-TN-02869

Remote sensing Analysis of Water Quality in Four Waterbodies of Latin America

Authors:
Ivan Lalovic, Fernando Miralles-Wilheim, Philipp Grötsch, Sara de Moitié, Adam Belmonte, Jihoon Lee, Raúl Muñoz Castillo, Cristina Mecerreyes, Henry Moreno, Marcello Basani, Maria Julia Bocco, Amalia Palacios, Gustavo Gonnelli, Eduardo Bogado, Javier Grau Benaiges

Editors:
Eveline Vásquez-Arroyo, Jose Rosales

Inter-American Development Bank
Water and Sanitation Division

December 2023

Remote sensing Analysis of Water Quality in Four Waterbodies of Latin America

Authors:
Ivan Lalovic, Fernando Miralles-Wilheim, Philipp Grötsch, Sara de Moitié, Adam Belmonte, Jihoon Lee, Raúl Muñoz Castillo, Cristina Mecerreyes, Henry Moreno, Marcello Basani, Maria Julia Bocco, Amalia Palacios, Gustavo Gonnelli, Eduardo Bogado, Javier Grau Benaiges

Editors:
Eveline Vásquez-Arroyo, Jose Rosales

Inter-American Development Bank
Water and Sanitation Division

December 2023

Cataloging-in-Publication data provided by the
Inter-American Development Bank
Felipe Herrera Library
Remote sensing analysis of water quality in four water bodies of Latin America / Ivan Lalovic, Fernando Miralles-Wilheim, Sara de Moitié, Philipp Grötsch, Adam Belmonte, Jihoon Lee, Raúl Muñoz Castillo, Cristina Mecerreyes Espinosa, Henry Moreno, Marcello Basani, Maria Julia Bocco, Amalia Palacios, Gustavo Gonnelli, Eduardo Bogado, Javier Grau Benaiges.
p. cm. — (IDB Technical Note ; 2869)
Includes bibliographical references.
1. Water quality-Latin America. 2. Remote-sensing images-Latin America. 3. Water quality-Technological innovations-Latin America. I. Lalovic, Ivan. II. Miralles-Wilhelm, Fernando. III. Grötsch, Philipp. IV. Moitié, Sara de. V. Belmonte, Adam. VI. Lee, Jihoon. VII. Muñoz-Castillo, Raúl. VIII. Mecerreyes, Cristina. IX. Moreno, Henry. X. Basani, Marcello. XI. Bocco, María Julia. XII. Palacios, Amalia. XIII. Gonnelli, Gustavo. XIV. Bogado, Eduardo. XV. Grau, Javier. XVI. Inter-American Development Bank. Water and Sanitation Division. XVII. Series.
IDB-TN-2869

Keywords: Innovation, Water Quality, Remote Sensing, Satellite-Imagery-Based Data, COVID-19

JEL Code: I14, I18, I31, I38, Q10, Q25, Q55, Q56, R20

http://www.iadb.org

Remote Sensing Analysis of Water Quality in Four Water Bodies of Latin America

Authors:

Ivan Lalovic, Fernando Miralles-Wilheim, Sara de Moitié, Philipp Grötsch, Adam Belmonte, Jihoon Lee, Raúl Muñoz Castillo, Cristina Mecerreyes Espinosa, Henry Moreno, Marcello Basani, Maria Julia Bocco, Amalia Palacios, Gustavo Gonnelli, Eduardo Bogado, Javier Grau Benaiges.

Editors:

Eveline Vasquez Arroyo, Jose Daniel Rosales

2023

IDB

Table of Contents

Remote Sensing Analysis of Water Quality in Four Water Bodies of Latin America

Authors: *Ivan Lalovic, Fernando Miralles-Wilheim, Sara de Moitié, Philipp Grötsch, Adam Belmonte, Jihoon Lee, Raúl Muñoz Castillo, Cristina Mecerreyes Espinosa, Henry Moreno, Marcello Basani, Maria Julia Bocco, Amalia Palacios, Gustavo Gonnelli, Eduardo Bogado, Javier Grau Benaiges.*

Editors: *Eveline Vasquez Arroyo, Jose Daniel Rosales.*

JEL codes: *I14, I18, I31, I38, Q10, Q25, Q55, Q56, R20.*
Keywords: *Innovation, Water Quality, Remote Sensing, Satellite-Imagery-Based Data, COVID-19*

Abstract

The pilot study introduces remote sensing methods for monitoring water quality to measure, understand, and manage impacts on vulnerable water bodies that are part of the IDB's Water and Sanitation portfolio. The water bodies selected for this study include: Guanabara Bay in Río de Janeiro, Brazil; Lake Titicaca in Bolivia and Peru; Ypacaraí Lake near Asunción, Paraguay; and the Río Reconquista Basin near Buenos Aires, Argentina. This study focuses on the development and implementation of an automated remote sensing data processing chain enabling detection of phytoplankton abundance (chlorophyll-a) as a proxy for pollution by organic and inorganic nutrients, as well as sediments (and turbidity or water 'clarity'), which are the major water quality issues identified across the IDB's Water and Sanitation portfolio. In addition to providing a baseline assessment of water resources at four select locations over time, the collected remote sensing data will be used to rapidly assess changes in water quality conditions resulting from socioeconomic changes introduced by local and regional responses to the Covid-19 pandemic and associated lockdown conditions. Remote sensing applied to water quality monitoring is a valuable emerging technology that can provide geospatial data about water quality and nutrient, bacterial, and industrial pollution from urban and rural sources. The methodology presented in this paper uses cloud computing, which allows rapid monitoring deployment and scalable coverage across numerous watersheds and geographies. Although this paper presents a comprehensive analysis of this entirely new source of water quality data across the sites and locations of interest, a more detailed analysis can be performed by examining different timeframes (e.g., entire data set or monthly aggregates) within these watersheds. Additional insights may be revealed by further combining the water quality data sets of this work with other sources of information, including local sensors, information from water and sanitation utilities, and a more detailed analysis of the timing of location conditions and their local impacts.

Abbreviations

ANOVA: Analysis of Variance

FNU: Formazin Nephelometric Units

IDB: Inter-American Development Bank

NASA: National Aeronautics and Space Administration

NDCI: Normalized Difference Chlorophyll Index

RBINS: Royal Belgian Institute of Natural Sciences

RRS: Remote Sensing Reflectance

RS: Remote Sensing

TSM: Total Suspended Matter

VG: Virtual Gauge

WQ: Water Quality

1

INTRODUCTION

Guanabara Bay

1. Introduction

1.1. Study Overview

This study, supported by the Inter-American Development Bank (IDB), introduces remote sensing methods for monitoring water quality (WQ) in support of measuring, understanding, and managing impacts in sensitive water bodies that are part of IDB's Water and Sanitation portfolio. The methods used enable systematic and scalable monitoring, analytics, and reporting about water quality or the water resource management portfolio, enhancing the effectiveness of tactical and strategic decision-making. This study focuses on the development and implementation of an automated remote sensing data processing chain to enable detection of sediments (or turbidity) and phytoplankton abundance as a proxy for pollution by organic and inorganic nutrients, which are the major water quality issues identified across the IDB's Water and Sanitation portfolio.

The monitoring and analytical tools demonstrated here provide decision makers and stakeholders with a new and comprehensive basis of measurement, as well as historical trends that can be used to inform about impact or progress monitoring for existing projects. The tools can also provide data to inform future water and sanitation investments aimed at improving water quality. Importantly, this study also provides a retrospective dataset against which can be compared the economic effects felt by varying Covid-19 lockdown measures. The data sets resulting from this study can further be compared with other socioeconomic, land-use, and water and sanitation utilization datasets to assess both the near-term, event-based changes such as the onset of Covid-19 restriction measures, or longer-term impact assessments.

Data production was tailored to specific reservoir, river, and estuarine systems of interest to stakeholders and thus provides a comprehensive analysis and dataset for a suite of water quality parameters. Additionally, this pilot study leverages the historical remote-sensing data archives to provide a baseline trend and variability assessment for water quality within these watersheds.

The water bodies selected for this study are as follows:

- **Guanabara Bay** in Río de Janeiro, Brazil
- **Lake Titicaca** in Bolivia and Peru
- **Ypacaraí Lake** near Asunción, Paraguay
- **Río Reconquista Basin** near Buenos Aires, Argentina

Finally, this study helped build capacity and strengthen activities undertaken by IDB staff in the country offices and their partner water managers in their use of remote sensing and GIS tools to improve water quality management.

2

METHODOLOGY

Lake Titicaca

2. Methodology

2.1. Remote-Sensing Datasets

At the core of this pilot study is a dense satellite time series dataset continuously collected over each of the four sites since early 2016. The two Sentinel 2 satellites orbit asynchronously to provide a new image of a location on the earth's surface every five days at the equator (two to three days at mid-latitudes). Each image has 13 unique spectral bands available in a resolution of 10-60m, depending on the band. These multi-spectral images provide a snapshot of the earth's surface beyond the visible red, green, and blue spectral bands available from a typical consumer-grade digital camera image. For example, the amount of water present in vegetation canopies can be calculated using spectra invisible to the human eye, the near infrared and shortwave infrared bands on Sentinel 2A (8A, 11, and 12). Satellite imagery datasets are acquired from the European Space Agency's Sentinel 2 A and B platforms, which can produce a high-resolution (10-20 m) multispectral (490-865 nm) image at the same location on Earth every five days. These imagery data are distributed free for public use and are used as the starting point for the satellite data processing methodology. This methodology ingests the raw top-of-atmosphere imagery, corrects for atmospheric effects, calculates a suite of WQ metrics, and creates a data repository for use across different display and analysis platforms. For this pilot study, three different WQ metrics are calculated and used for the assessment of each water bodies.

Chlorophyll-a measures the concentration of phytoplankton growing in the water and is expressed in milligrams per cubic meter (mg/m^3). Water quality problems associated with changes in this water quality parameter are typically caused by nutrient pollution.

Turbidity measures the optical clarity of water and is expressed in Formazin Nephelometric Units (FNU).

Total Suspended Matter measures the concentration of fine particles, both inorganic and organic, that are suspended in the water and is expressed in units of grams per cubic meter (g/m^3). Water quality problems associated with changes in this water quality parameter are typically caused by sediment pollution.

The three WQ metrics were used for rapid monitoring deployment and scalable coverage across the four selected watersheds and geographies. More water quality datasets with additional socioeconomic information may unravel the causes and dynamics among the WQ metrics as well as sources of pollution in the selected water bodies. All resulting WQ product datasets are geo-referenced, cloud-screened, and adjusted to account for localized water extent changes over time.

2.2. Adaptation of NASA's Ocean Color Radiometry

Figure 1 illustrates the basis of the methodology used for processing remote sensing observations into water quality estimates. NASA and other space agencies have established protocols for how this is done, and following NASA nomenclature these top-of-atmosphere corrected images are referred to as processing level "L0".

To make these images useful for calculating water quality parameters, the images must undergo a process that removes the effects of the atmosphere present between the satellite sensor and the earth or water surface. This process, termed atmospheric correction, implements a series of algorithms to reduce or eliminate the effects of atmospheric absorption and backscatter on the image, yielding a more accurate representation of the earth's surface. The resulting images contain values for the remote sensing reflectance (abbreviated as Rrs) of the water body, which are referred to as "L1" in the commonly adopted NASA nomenclature. These processed images can then be used to derive a variety of data products.

Reflectance data processing approaches commonly rely on atmospheric correction processes based on open-source methods developed for inland and coastal water applications. Examples include the Royal Belgian Institute of Natural Sciences' (RBINS) Acolite processor and the National Aeronautics and Space Administration's (NASA) SeaDAS processor. The full image collections, also referred to as archives, containing the atmospherically corrected imagery and Rrs values, are used to calculate the three WQ products in this pilot study: chlorophyll-a, suspended matter, and turbidity concentrations.

We derived the following WQ products by applying relatively standard algorithms used in the open scientific literature and developed specifically for detecting the makeup of inland coastal waters.

Figure 1: Depiction of remote sensing data processing from satellite imagery (reflectance) applied to water quality estimates

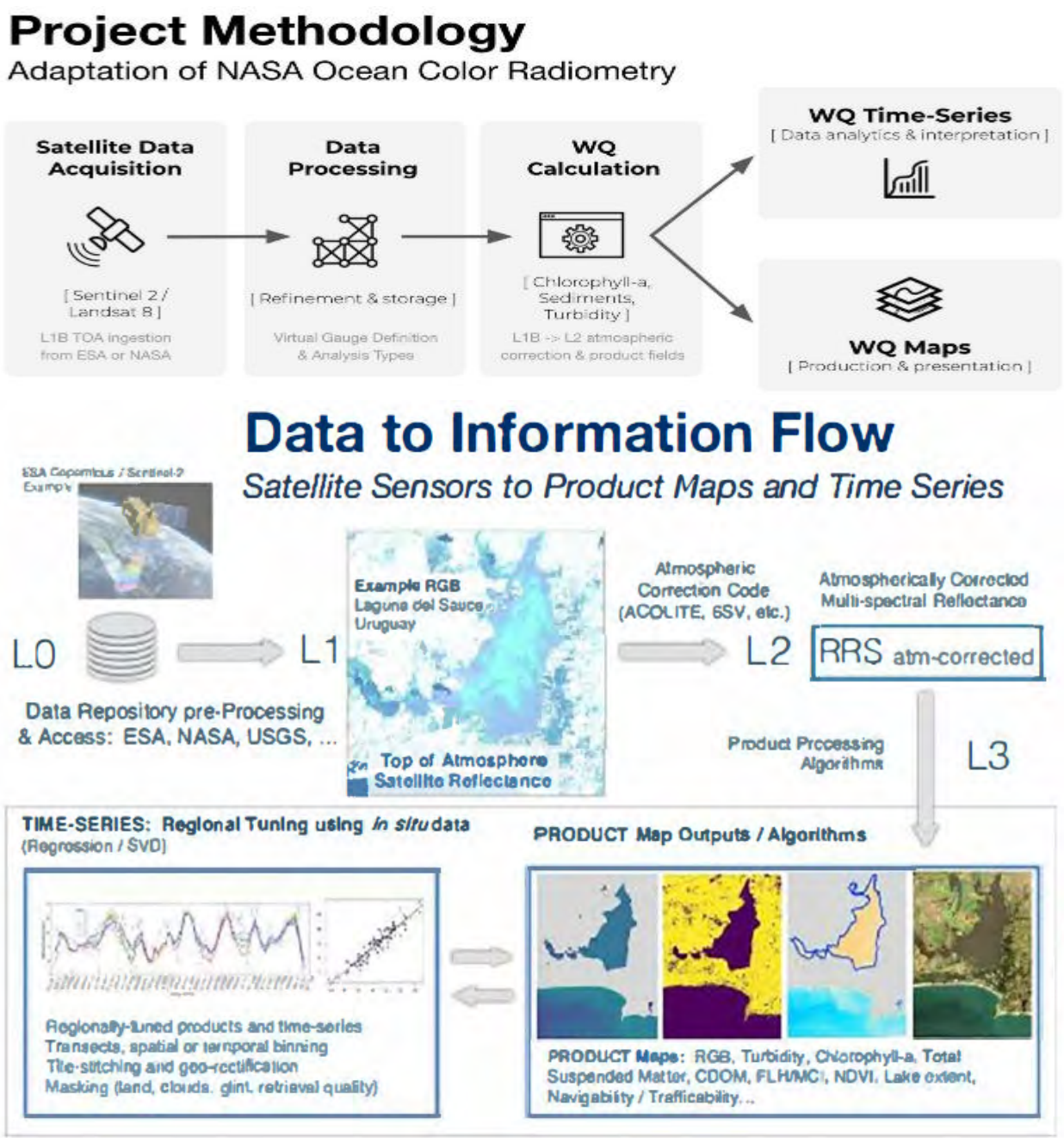

The full image collections, also referred to as archives, contain the atmospherically corrected imagery and Rrs values, which are used to calculate the three water quality (WQ) products in this pilot study: chlorophyll-a, suspended matter, and turbidity concentrations.

- Chlorophyll-a concentrations, which are measured in milligrams per cubic meter (mg/m^3), are calculated using the normalized difference chlorophyll index (NDCI) developed by Mishra[1].
- The NDCI algorithm can be used to detect algae concentrations and blooms using the red and red-edge spectral bands.
- Suspended matter and turbidity concentrations are measured in grams per cubic meter (g/m^3) and Formazin Nephelometric Units (FNU), respectively, and are both derived from the methodology developed by Nechad et al.[2] for detecting total suspended matter (TSM) concentrations on the water surface.

It is important to note that the data in this report is not calibrated or validated against ground measurements, which is an effort deemed out of the scope of this pilot, in part due to inconsistent availability of water quality data across the four pilot sites. The analyses used in this pilot study relied on the pixel-wise time series data extracted from the entire water surface across each site. Having datasets that were dense in both the spatial (10 m pixels) and temporal (one new image roughly every five days) dimensions facilitated analyses that could focus on establishing WQ baselines, quantifying changes in temporal trends, and illustrating patterns in spatial distributions. Trends over time and within seasons were established using simple time series plots constructed from the average or median WQ data product value across the entire water surface or else constrained to virtual gauge locations. Moving average filters were applied to time series data to both smooth spikes and interpolate across small gaps.

1 Mishra S., & Mishra, D.R. (2012). Normalized difference chlorophyll index: A novel model for remote estimation of chlorophyll-a concentration in turbid productive waters. Remote Sensing of Environment 117(3): 394-406.

2 Nechad, B., Ruddick K.G., & Park, Y. (2010). Calibration and validation of a generic multisensor algorithm for mapping of total suspended matter in turbid waters. Remote Sensing of Environment 114(4): 854-866.

2.3. Spatial and Temporal Data Analyses

Virtual Gauges

A virtual gauge is a specific geographic region of interest in which water quality parameters are temporally assessed in greater detail than viable across the entire water body. The goal of establishing virtual gauge locations is to extract data that enables rapid, flexible, and relevant investigation into areas where known WQ issues exist.

To establish a virtual gauge location, information from local experts and the scientific literature about where WQ issues originate or tend to occur were collected first. Examples of this information include official WQ sampling locations, informal reports from citizens, known point source polluters, areas where rivers meet a reservoir, or locations of critical infrastructure (e.g. drinking water or hydropower intake locations). Then, a spatially referenced area is created that reflects both the research and a statistically relevant pixel sample size. In this way, virtual gauges allow users to generate time series for any point or area that is of interest on the data maps, as if we had placed a gauge there physically.

In this pilot, virtual gauge locations depended on feedback from IDB country office staff members who are managing projects in the selected water bodies, with a preference for areas close to densely populated regions and at least 50 meters across in rivers. Those at Ypacaraí Lake were selected with a focus on being directly downstream from densely populated areas where tourism dominates (virtual gauges 2 and 4), as well as at the natural in-flow and out-flow locations (virtual gauges 1 and 3). At Guanabara Bay, virtual gauges were established at the major outflow points from heavily populated and polluted waterways (virtual gauges 1, 2, 3, and 4), as well as at points where natural flow patterns can be observed (virtual gauges 4 and 5). In the Río Reconquista Basin, virtual gauge locations 1, 2, and 3 were selected because they can summarize in-flow/out-flow activity within the Río Reconquista basin, while virtual gauges 4 and 5 were used as auxiliary measures of activity in the adjoining basins within the Buenos Aires metropolitan area. At Lake Titicaca, all virtual gauges were established based on being downstream from some significant population, as well as being located within the shallower and geographically isolated bays that characterize the lake.

Figure 2: Virtual gauges in each water body

Ypacaraí Lake

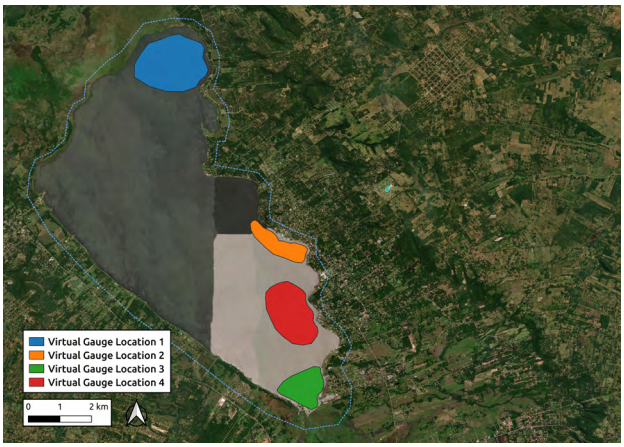

- 4 locations of interest defined (=virtual gauges)
- Central Department, Paraguay

Guanabara Bay

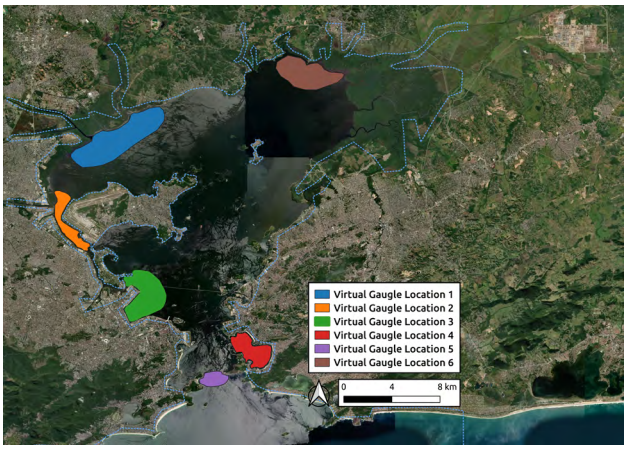

- 6 locations of interest defined (=virtual gauges)
- Río de Janeiro, Brazil

Río Reconquista Basin

- 5 locations of interest defined (=virtual gauges)
- Buenos Aires, Argentina

Lake Titicaca

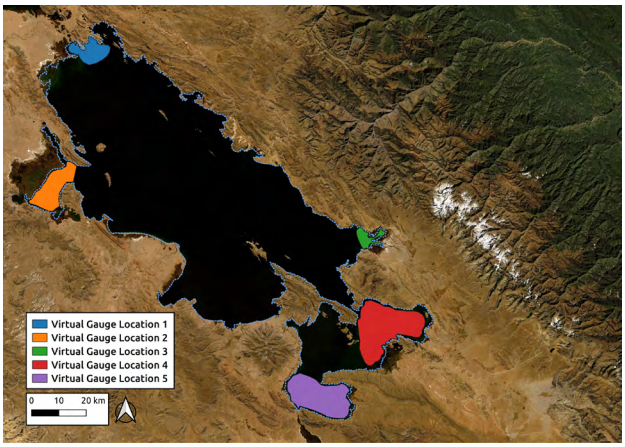

- 5 locations of interest defined (=virtual gauges)
- Bolivia and Peru

2.4. Seasonal Trends

Maps illustrating the average seasonal changes across the entire water body were created to better understand the seasonal effects on water quality parameter values. First, water quality values across the full archival time series were grouped into three-month intervals: December through February; March through May; June through August; and September through November. Then, values were averaged through time to produce maps that highlight seasonal differences. This allows for identification of periods during the year or location within the water body where trends are noticeable, providing a method to link hydrological and land processes, or prevailing meteorological conditions. Seasonal and meteorological drivers not only impact urban and rural runoff; they can also influence hydro-dynamics (water mixing), including flooding, storm surge, sewage flows, and light available for photosynthesis, as well as photochemical processes within the watershed.

Figure 3: Spatial mapping of seasonal trends of suspended matter concentrations (g/m3) in Lake Titicaca

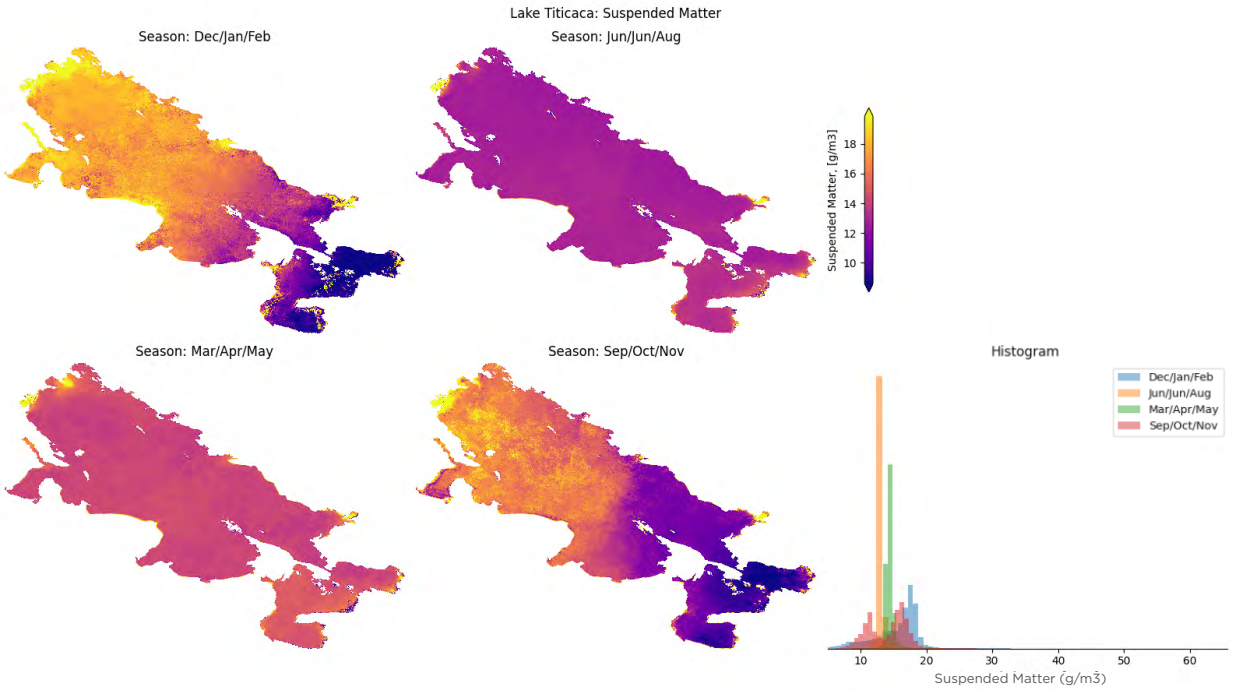

Data on water quality time series split by year are plotted to further illustrate the differences within seasons and across years. Plots are produced for the entire water body as well as for each virtual gauge location. Such plots can be produced for sub-regions of a water body or specific virtual gauge locations.

2.5. Water Quality Changes from Covid-19 Lockdown

Changes to WQ stemming from Covid-19 lockdown restrictions were assessed from Gybe's remote-sensing data using a series of simple one-way analysis of variance (ANOVA) tests. Differences in pre- and post-Covid-19 conditions were tested for each WQ metric at each virtual gauge location, with pre-Covid-19 lockdown defined as all-time series data before March 19, 2020. While the timing and length of lockdown measures varied across the sites (see Appendixes), a general assumption that lockdown measures ebbed and flowed starting in March 2020, combined with a seasonally-based division of data, allowed for an as accurate as possible approach to comparing pre- vs. post-Covid-19 trends. Both pre- and post-Covid-19 datasets were separated into three-month seasons, with tests performed on each season to control for seasonal variations. Significant differences between conditions were recorded with a 'p-value' less than 0.05.

Separately, an assessment of Covid-19 lockdown-related differences in WQ was conducted across the entire water body to illustrate general trends not associated with virtual gauge locations. For this, pixel-wise differences were calculated across the entire water body using images downsampled to 30 m pixels. The resulting images illustrate where changes in WQ are observable. Here, the pixels where statistically significant differences that coincide with the period pre- and post-onset of Covid-19 are color coded; blue areas indicate locations where an increase in the water quality parameter is observed and red indicates areas where specific water quality parameters are lower. As expected, these changes have some seasonal patterns that could be enhanced by seasonal environmental differences or the timing and severity of lockdown requirements and resulting changes in economic activity.

2.6. Long-term Trends (Mann-Kendall Trend Test)

A seasonally adjusted Mann-Kendall Trend Test (Hirsh et al., 1982) was applied to virtual gauge locations to identify whether a water quality parameter is increasing or decreasing over time in a specific area. First, the median water quality parameter value is calculated across a virtual gauge location for each image date. Then, a Mann-Kendall test is applied to the full archival time series, which provides the direction, magnitude, and statistical significance of potential trends at that location. The outcome indicates whether the time series data at that location has a consistent increasing or decreasing trend. This statistical assessment is particularly useful to understand the underlying variability and longer-term trends at specific locations in which Covid-19 event-driven changes, are observed.

Figure 4: Plot showing the Mann-Kendall-derived long-term trend calculated at virtual gauge locations in Lake Titicaca from 2017 to 2021. Here, a significantly decreasing trend in chlorophyll-a concentrations was found at virtual gauge location 2 (VG-2)

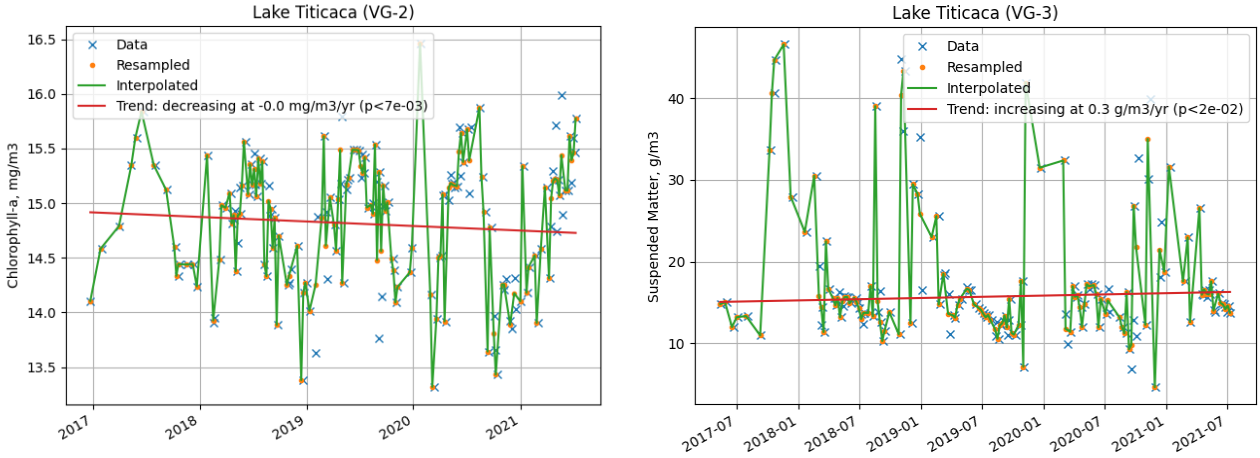

2.7. Spatial Variation Maps

Variation maps were created for each water body and water quality parameter to quantify where water quality values are consistently high, low, and have high variability over time. This process calculates the median, standard deviation, and coefficient of variation on a pixel-wise basis over time. The product is a map that shows the spatial distribution of these summary statistics over time. These maps can be used to locate areas that stand out with consistently different water quality patterns or areas with high variability. Either of these areas could be locations that are valuable indicators of important processes or can be used as locations for more detailed monitoring.

Figure 5: A set of variation maps showing the spatial distribution of chlorophyll-a concentrations across Guanabara Bay, Brazil throughout the entire time series archive

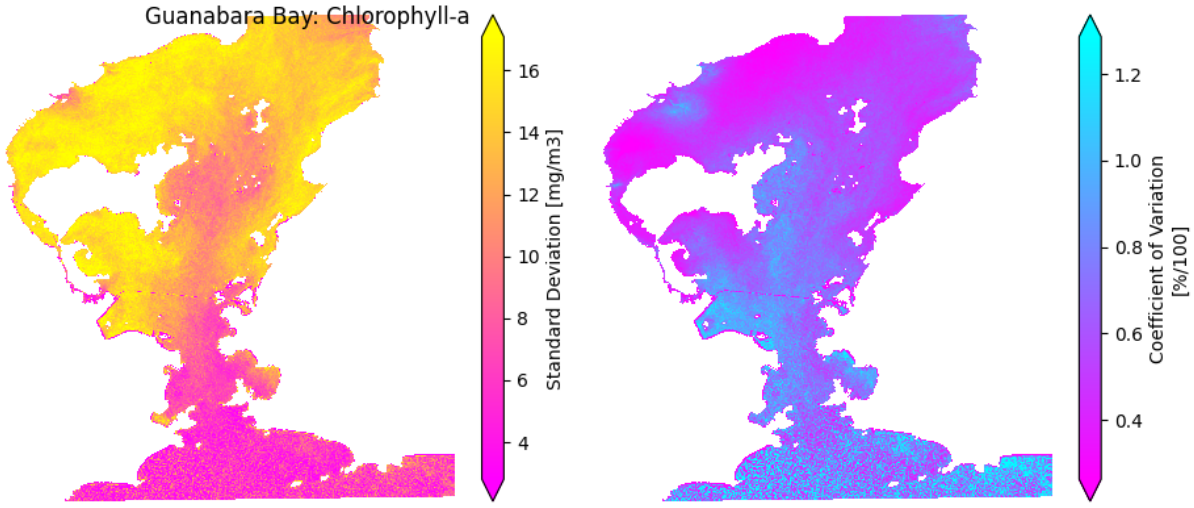

2.8. Spatial Trend Maps

Next, extending the concept of variation maps, trend maps were created to visualize where temporal trends in water quality parameters are occurring. First, data across the entire water body is spatially binned by averaging to approximately 100m resolution. Then, a linear regression is applied along the temporal axis for each bin; a three-sigma outlier filtering process is used to remove outliers. Finally, linear trends are visualized on a map, where statistically significant (p-value below 5%) values are colorized based on direction and intensity. Similar to the spatial statistics maps, colorized areas can be used to understand areas or locations where long-term trends indicate a linear trend in underlying water quality over multiple years, showing increasing environmental pressures on ecosystems, or successful implementation of policies, land-use practice, or water and sanitation projects.

Figure 6: Maps of Ypacaraí Lake showing the areas in which there are consistently lower suspended matter concentrations. In this example, blue areas depict 'cold spots', with the darker pixels indicating a stronger trend. These areas could be related to clearwater inputs or more stagnant water causing less sediment resuspension

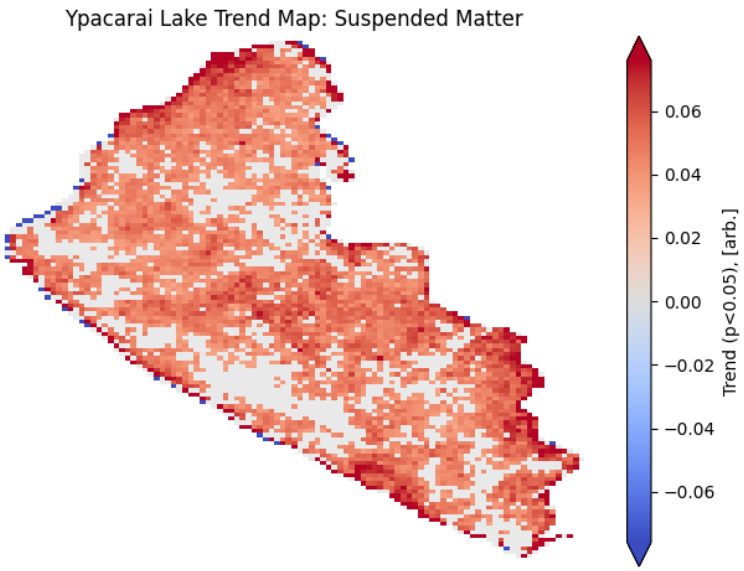

3

RESULTS AND DISCUSSION

Ypacaraí Lake

3. Results and Discussion

3.1. Guanabara Bay, Brazil

Guanabara Bay is a 384 km^2 area surrounded by several of Brazil's major metropolitan areas and roughly 8.6 million people, many of whom reside in the city of Río de Janeiro. About 84% of the bay is less than 10m deep, with the remaining portion a deep main channel that leads out to the Atlantic Ocean; these properties hamper internal circulation of water within the bay (Kjerfve et al., 1997). Significant land-use change away from the natural estuarial ecosystems to heavy industrial and residential use has led to widespread ecological degradation in water quality in the bay (Fisatrol et al., 2015). Unfiltered organic waste from sewage outfalls draining dense residential development has led to severe eutrophication and a significant decline in marine life (Carreira et al., 2002; Nepomuceno et al., 2006). High chlorophyll-a levels tend to be observed at locations draining dense residential and industrial development, which correspond to virtual gauge locations 1, 2, and 3 (Figure 7). Patterns at these locations also follow a seasonal trend, with higher concentrations occurring during warmer and wetter months, especially November through March for locations 2 and 3, during a period of higher solar radiation in the southern hemisphere. This data set could be used to design a monitoring plan to better understand key sources of nutrients and organic matter resulting in eutrophication. For further explanation, please see Full Analysis of Guanabara Bay.

Figure 7: Annual trends in chlorophyll-a concentrations at virtual gauge locations 1, 2, and 3 across Guanabara Bay

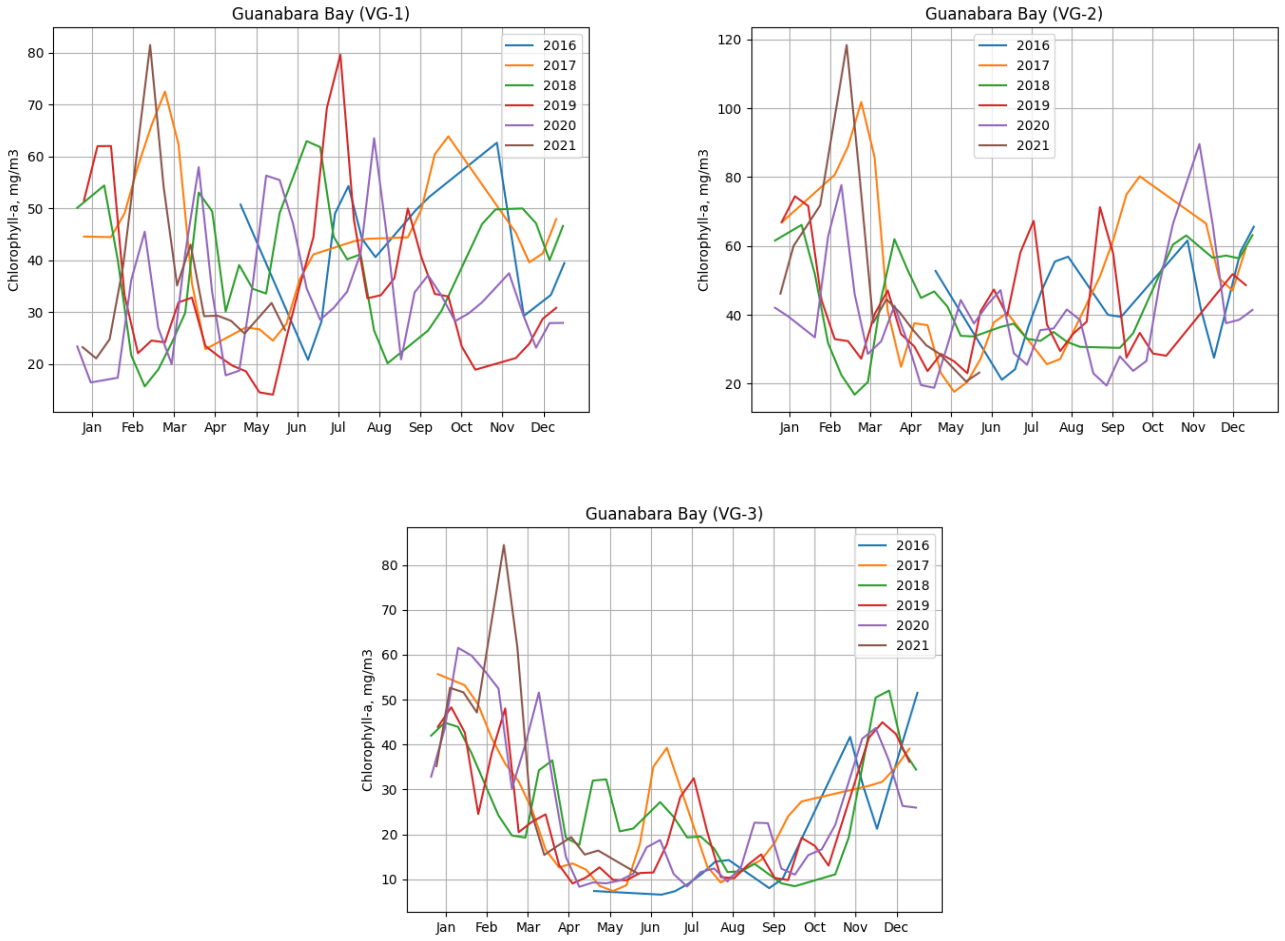

This shows a strong seasonal pattern where algae blooms are prevalent in the southern hemisphere summer, and higher amounts of photosynthetic radiation and higher nutrient runoff occur.

As an outlet for several major unobstructed rivers, annual trends in turbidity and suspended matter concentrations align with the rainiest months, from December to March, and are particularly noticeable at virtual gauge location 6 (Figure 8).

Figure 8: Panel A shows the annual trends in turbidity across the entire Guanabara Bay. Higher levels starting in November appear to correspond with higher precipitation inputs to the watershed. Panel B shows the same trends at virtual gauge location 6, where many rivers empty into the bay

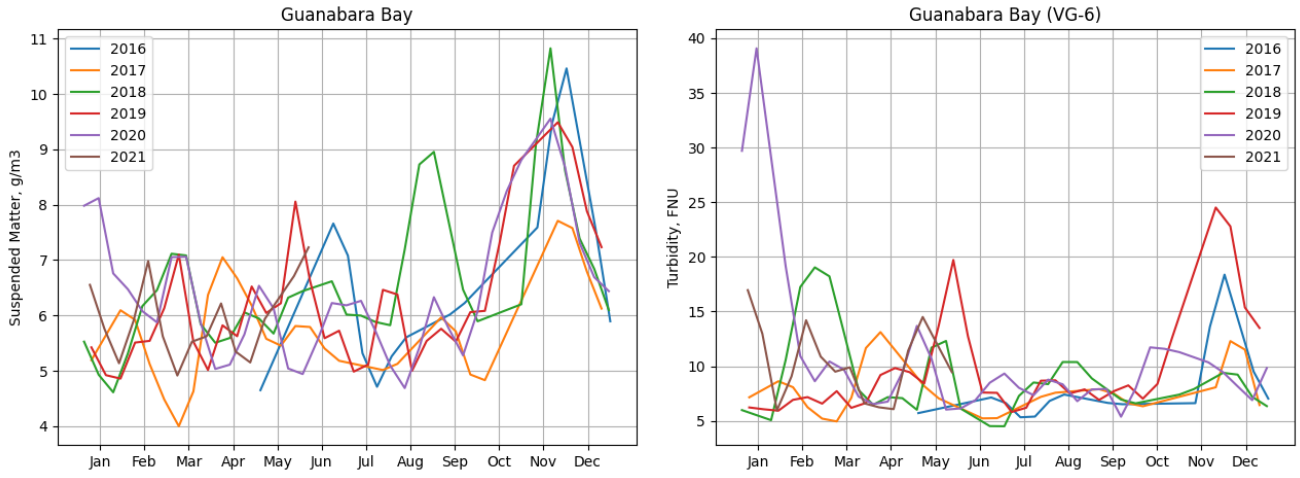

There were significant differences in WQ metrics that correspond with the general timing of Covid-19 lockdown measures at several virtual gauge locations in Guanabara Bay. Lockdown measures affecting Río de Janeiro are summarized in Appendix 4 and were limited to the month of May 2020 for the context of this study. Overall, there were few instances of statistically significant changes in WQ metrics at virtual gauge locations (Table 1); however, significant trends at these locations are further observed and corroborated across the entire water surface (Figure 9). In particular, post-Covid-19 lockdown conditions show overall reductions in chlorophyll-a concentrations across much of Guanabara Bay, with significant reductions at virtual gauge locations 1 and 6. Reductions in chlorophyll-a concentrations at virtual gauge 1 at the location of the outlet of the heavily polluted Río Iguazú, could be caused by changes in industrial and residential discharges at varying stages of lockdown restrictions. However, at virtual gauge location 4, the increase in chlorophyll-a concentrations during the active lockdown period (Mar/Apr/May 2020) could be tied to increased residential effluent from people being at home. Table 1 summarizes the locations with statistically significant ($p < 0.05$) differences between pre- and post-Covid-19 lockdown measures, with site-wide differences illustrated in maps of the entire water surface across the site (Figure 9).

Table 1: Locations with statistically significant ($p < 0.05$) differences between pre- and post- Covid-19 lockdown measures

Virtual Gauge #	WQ Metric	Months	Direction of Change (during the observed months)
1	Chlorophyll-a	Sep/Oct/Nov (2020)	Decrease
1	Chlorophyll-a	Dec/Jan/Feb (2020-2021)	Decrease
4	Chlorophyll-a	Mar/Apr/May (2020)	Increase
4	Susp. Matter & Turbidity	Dec/Jan/Feb (2020-2021)	Decrease
6	Chlorophyll-a	Dec/Jan/Feb (2020-2021)	Decrease

Figure 9: Pixel-wise differences between pre- and post-Covid-19 lockdown measures in chlorophyll-a (Panel A) and suspended matter (Panel B) concentrations across Guanabara Bay. Each 10m pixel depicts the difference in mean WQ metric values between the pre- and post-Covid-19 timeframes.

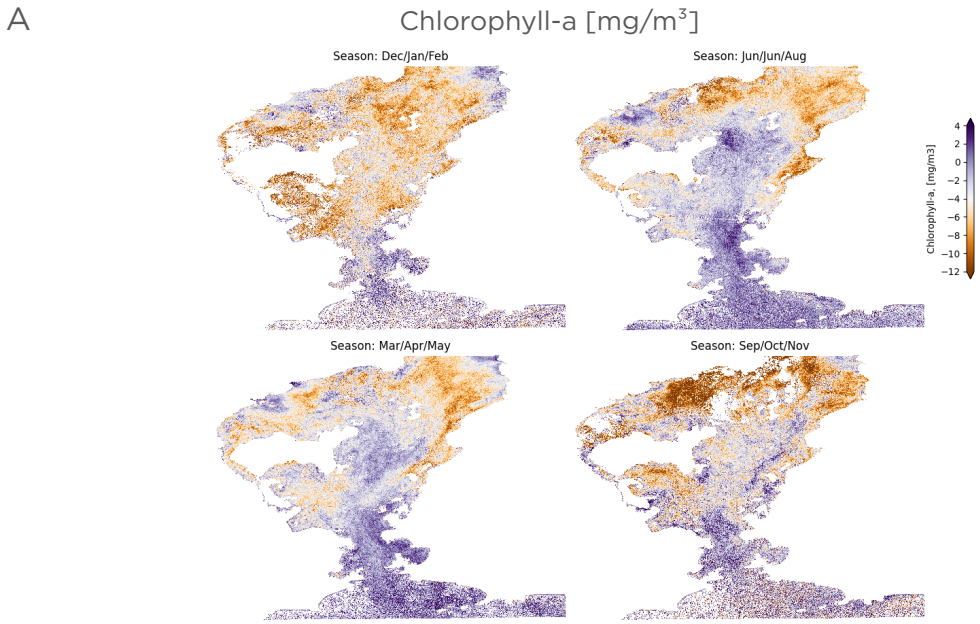

B

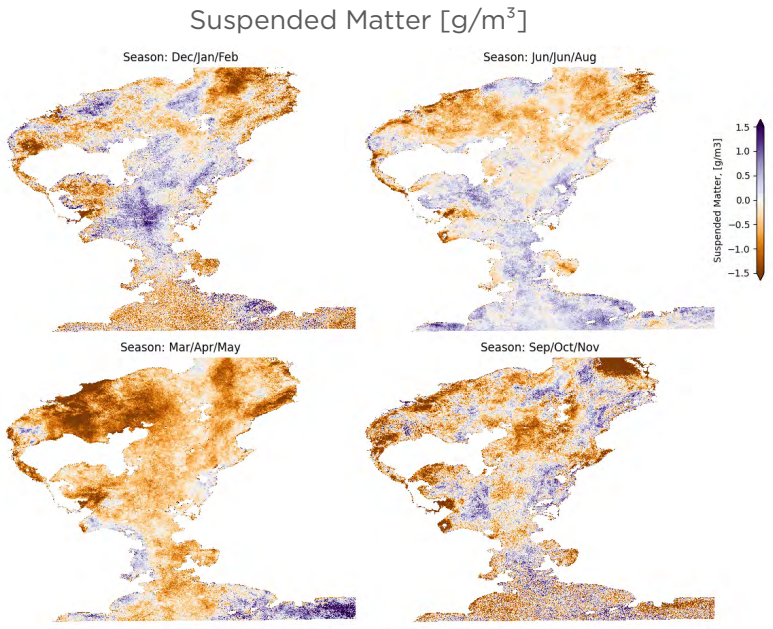

Overall, Figure 8 indicates that chlorophyll-a concentrations appeared to significantly decrease across the entire bay throughout the Covid-19 onset and lockdown timeframe, which could indicate generally lower nutrient levels across the bay. However, due to size and complexity of the inputs into the bay, pinning down the origin of these changes is less straightforward, and requires narrowing the analysis to areas where local and more detailed understanding of restrictions in place during Covid-19, assessing this information in concert with demographic and economic geospatial data. More variable conditions along the western shoreline near Río de Janeiro suggest that effects from lockdown measures can be localized and may be dependent on enforcement of and compliance with restrictions in these areas, coupled with quality of water and sanitation infrastructure in those locations. In particular, the area near virtual gauges 1 and 2 has opposing patterns in suspended matter concentrations between March/April/May and December/January/February. The decrease in suspended matter concentrations during March/April/May (2020) appears to correspond with the official lockdown period in Río de Janeiro (May 5 - May 24, 2020). Decreased suspended matter concentrations during this time may correlate with decreased industrial wastewater output. Meanwhile, the increases during December/January/February (2021) point to relaxed lockdown measures and increased activity overall (Appendix 4).

3.2. Lake Titicaca, Peru, and Bolivia

As the largest freshwater lake in South America, Lake Titicaca is integral to the high plateau regions of Peru and Bolivia, where much of the population depends on the lake for cultural, agricultural, and economic activities. Increased untreated outflows from industrial and residential development have compromised larger ecosystem health and led to binational government programs aimed at implementing sanitation projects at key places around the lake (Duquesne et al., 2021). In particular, the shallower areas in the southern (Río Katari outlet), far western (Puno Bay), far eastern (near Achacachi), and northern portions (Río Ramis) all are subject to decreased water quality and algal blooms (Cruz et al., 2010; Komárková et al., 2016). Consequently, higher chlorophyll-a concentrations are observed at virtual gauge locations that align with these shallower areas (Figure 9). Interesting to note is the strong seasonal variation at some locations, while others remain consistent throughout the years. Both the strong variation and consistency at these locations could be due in part to wind-driven water circulation patterns, from winds predominantly from the north and west. Similarly, these patterns are observed in turbidity and suspended matter concentrations at the same virtual gauge locations (Figure 11).

Figure 10: Full time series of chlorophyll-a values at all virtual gauge locations throughout Lake Titicaca

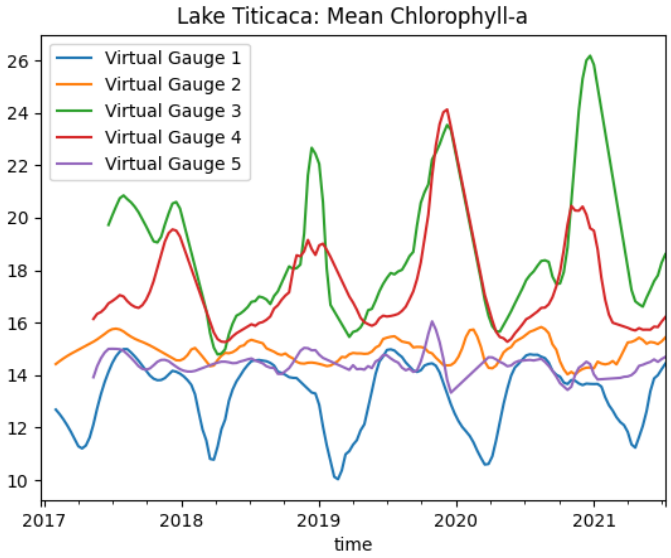

The strong seasonality in virtual gauges 1, 3, and 4 could be due in part to their locations downstream from significant population centers and the increased organic pollutants that might be running off from these locations, contributing to higher chlorophyll-a concentrations from algal blooms. The lack of strong seasonal signals at virtual gauge locations 2 and 5 could also be in part due to lower nutrient levels. In these locations, there is likely less wind-driven movement on the water surface, since the predominant wind direction is out of the west, which typically creates conditions well-suited for surface algal bloom formation.

Figure 11: Full time series of turbidity and suspended matter values at all virtual gauge locations throughout Lake Titicaca

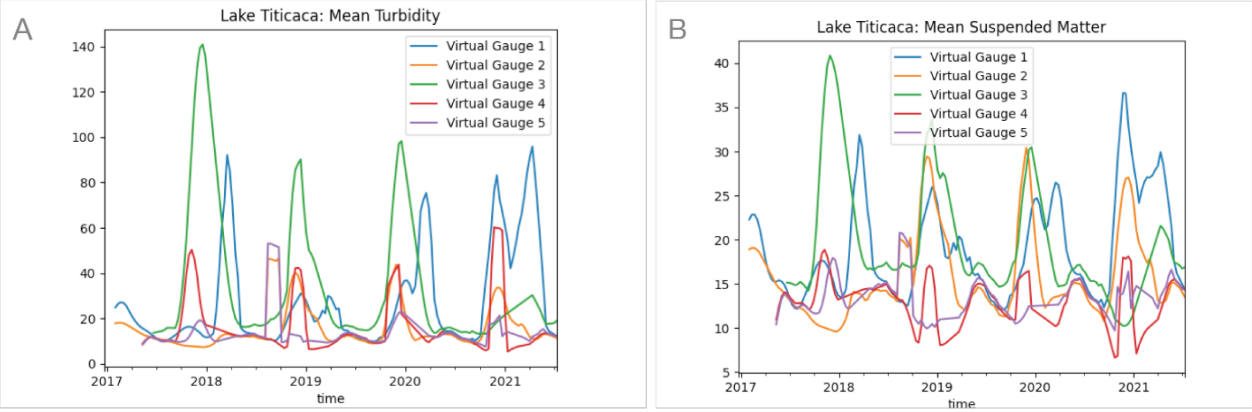

During the latter part of 2020 and into 2021, turbidity and suspended matter concentrations at virtual gauge location 3 decreased to below normal levels. This decrease also mirrored an increase in chlorophyll-a concentrations at that same location. This perhaps indicates that limited industrial activity contributed to a reduction in runoff, while increasing the likelihood of algal growth in clearer waters.

In the Lake Titicaca region, the only official Covid-19-related lockdown measures were in effect in La Paz/El Alto (virtual gauge location 4) during April-May 2020 (Appendix 3). There were significant differences in WQ metrics observed from Covid-19 lockdown measures at several virtual gauge locations in Lake Titicaca (Table 2); however, significant trends at these locations are further observed and corroborated across the entire water surface (Figure 12). In particular, post-Covid-19 conditions show isolated areas with clear changes in WQ metrics, and these areas tend to be downstream from larger population centers in La Paz, Achacachi, Desaguadero, and Puno. In addition to corresponding with the virtual gauge locations, these areas tend to be isolated from the main lake area and in bays and inlets. No significant effects on WQ metrics were observed, despite active lockdown measures in La Paz/El Alto during April-May 2020 (Appendix 3). However, there were significant differences found at adjacent virtual gauge locations (3 and 5) downstream of Achacachi and Desaguadero, respectively. An analysis about local implications of lockdown measures in terms of population movement and impacts on water and sanitation infrastructure utilization would help explain these differences. Table 2 summarizes the significant ($p < 0.05$) differences between pre- and post-Covid-19 lockdown measures, with site-wide differences illustrated in maps of the entire water surface across the site (Figure 12).

Table 2: Significant ($p < 0.05$) differences between pre- and post-Covid-19 lockdown measures

Virtual Gauge #	WQ Metric	Months	Direction of Change (during the observed months)
1	Chlorophyll-a	Dec/Jan/Feb (2020-2021)	Increase
2	Chlorophyll-a	Jun/Jul/Aug (2020)	Increase
2	Chlorophyll-a	Sep/Oct/Nov (2020)	Decrease
3	Chlorophyll-a	Mar/Apr/May (2020)	Increase
5	Susp. Matter & Turbidity	Dec/Jan/Feb (2020-2021)	Increase
5	Susp. Matter & Turbidity	Mar/Apr/May (2020)	Increase

Figure 12: Pixel-wise differences between pre- and post-Covid-19 lockdown measures in chlorophyll-a (Panel A) and suspended matter (Panel B) concentrations across Lake Titicaca

A

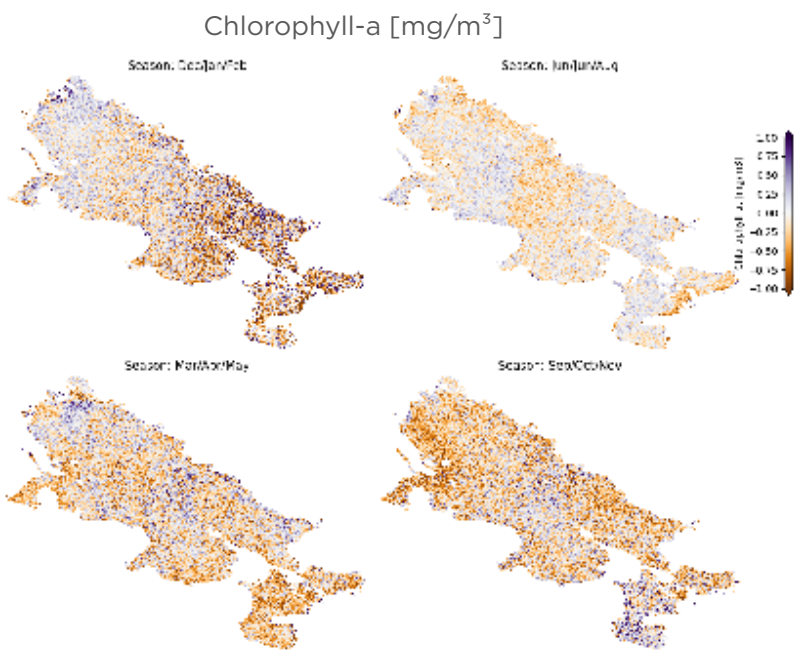

B

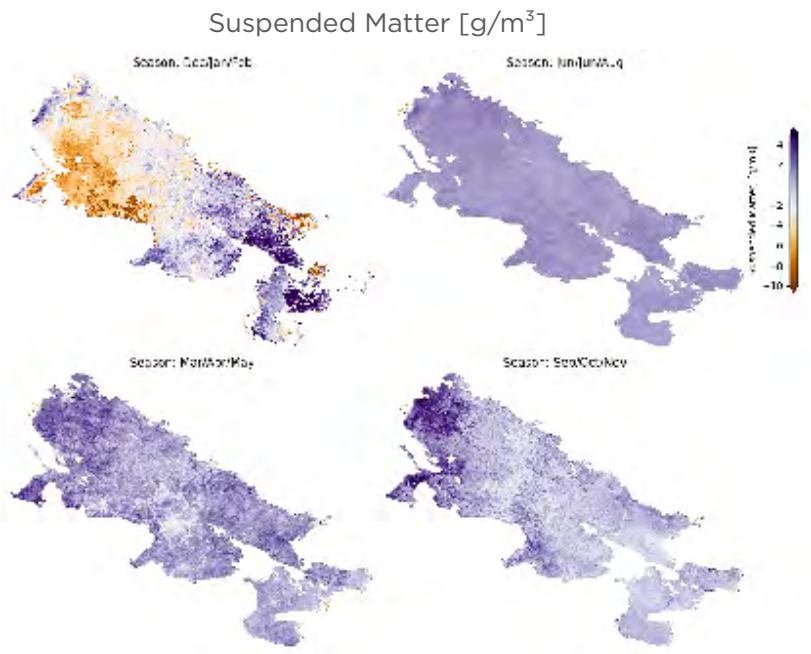

Each 10m pixel depicts the difference in mean WQ metric values between the pre- and post-Covid-19 timeframes. Few to no significant changes were observed across the entire lake from March through August. Then, from September to November, significant increases in suspended matter concentrations were observed near the areas that correspond with virtual gauges 1, 2, and 4. Following this, there was a significant decrease in suspended matter near virtual gauge locations 3 and 4 from December 2020 through February 2021.

Interestingly, at virtual gauge location 5, there was both an increase in pre- vs. post-Covid-19 changes to suspended matter and turbidity during March-May 2020 and December-February 2020-2021. This is also observed in the long-term trend found in the full time series data from the Mann-Kendall analysis (Figure 13) and further highlighted in the trend map surface (Figure 14).

Figure 13: Mann-Kendall trend analysis of suspended matter levels at virtual gauge location 5, which corresponds to the southwestern portion of Lago Menor

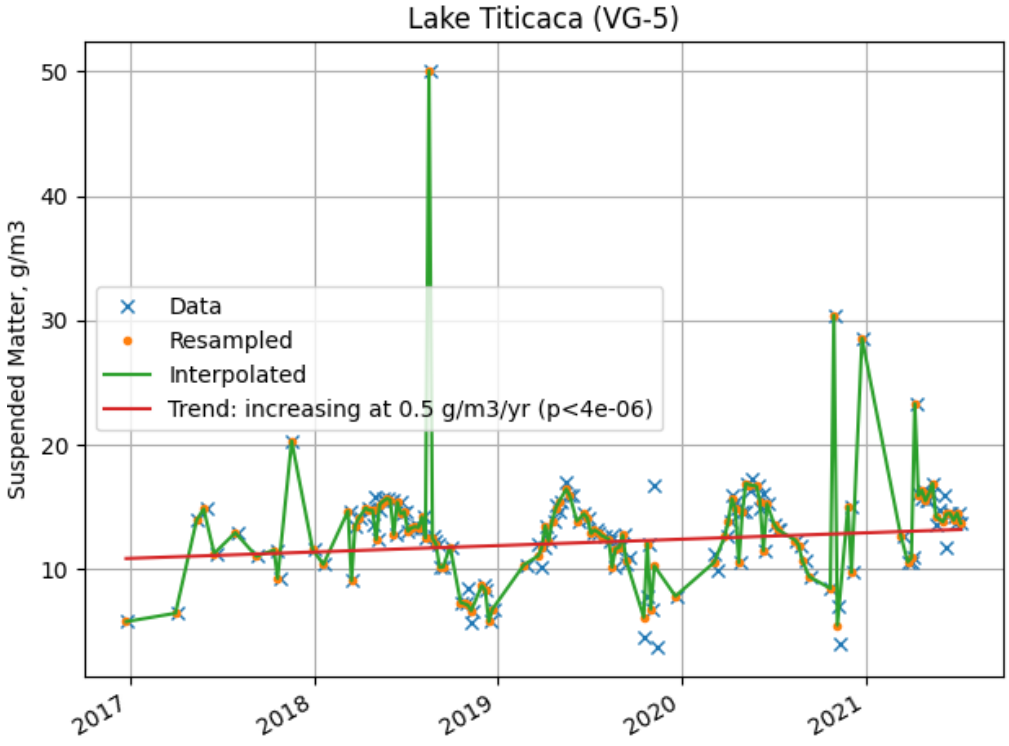

Figure 14: Trend map showing the direction and magnitude of the long- term trends in suspended matter across Lake Titicaca

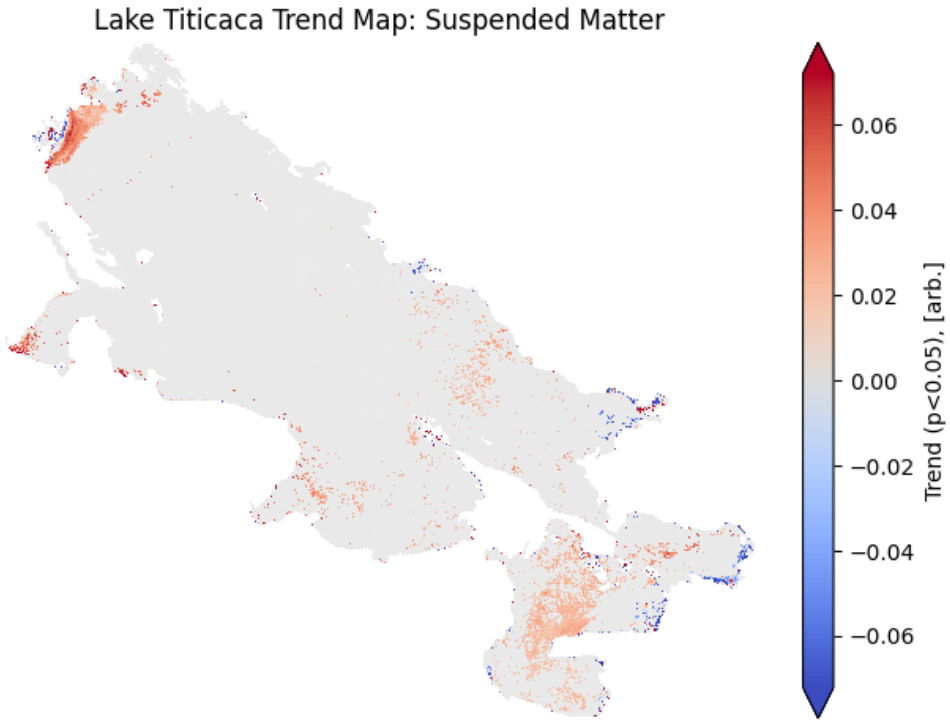

3.3. Río Reconquista Basin, Argentina

The Río Reconquista Basin houses around 11% of Argentina's population, comprising 33% of the Buenos Aires metropolitan area; as a result, it faces considerable pollution from industrial wastewater and untreated sewage from informal residential settlements (Castañé et al., 2006; de Cabo et al., 2000). Regional and international programs, including those funded by the Inter-American Development Bank (IDB), have implemented measures to improve both wastewater and flood control infrastructure throughout the basin (Janches et al., 2014). Importantly, this includes channelization of the Río Reconquista through the densely populated area between Roggero Dam (Lago San Francisco) and the Río Luján. While such channelization helps control flows from the dam through urban areas, it can also concentrate polluted runoff (Figure 15). Strong seasonal trends in all WQ metrics are observed across the entire site and are particularly pronounced at specific virtual gauge locations (Figure 16). To effectively monitor long-term and Covid-19 lockdown-related effects on WQ metrics across the entire region, the virtual gauges were established at strategic points. Starting with those specific to the Río Reconquista, virtual gauges 1-3 were established at Lago San Francisco, the lower section of Río Reconquista, and the outlet of Río Luján, respectively. To characterize the adjoining basins in the Buenos Aires metropolitan region, virtual gauges 4 and 5 were established at the outlet of the Matanza River and downstream from the city of La Plata, respectively. All virtual gauge locations were selected based on input from IDB stakeholders, size specifications (> 50m wide), and proximity to densely populated areas.

Figure 15: Full time series of chlorophyll-a (Panel A) and suspended matter (Panel B) concentrations across the Río Reconquista Basin

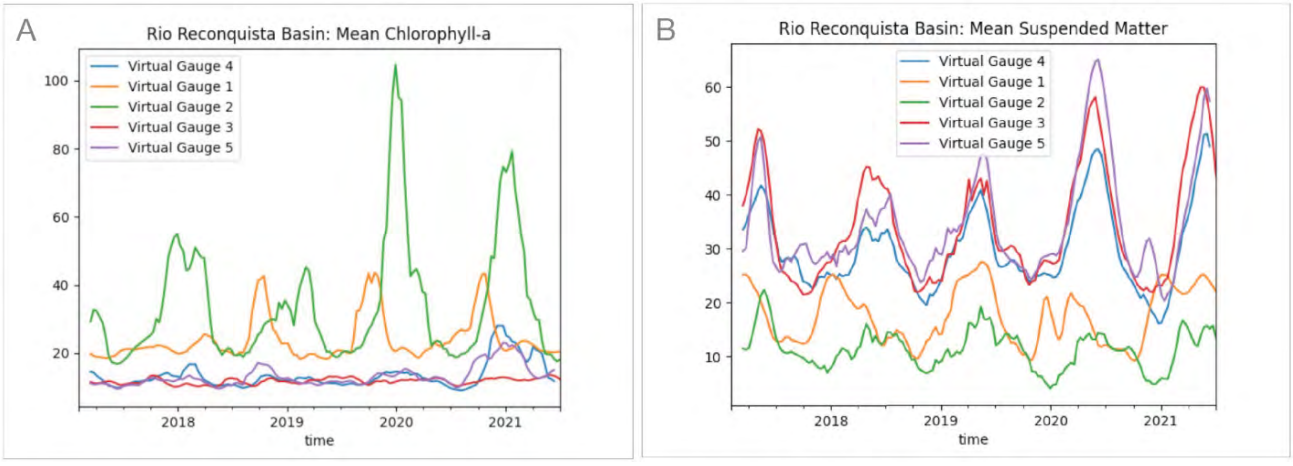

Each line corresponds to a different virtual gauge location. Interestingly, the conveyance of water through the Río Reconquista can be observed in the lag between water leaving Lago San Francisco (virtual gauge 1) and flowing through the confluence with the Río Luján (virtual gauge 2). The overall higher concentrations of chlorophyll-a at virtual gauges 1 and 2 (Panel A) are due to the greater input of nutrients that trigger algae growth from the urbanized watershed, coupled with a lower overall volume of water in this part of the system. The opposite effect is observed in suspended matter concentrations (Panel B), where the inherent presence of suspended sediments is higher at locations where water volume is greater and there are greater inputs from non-urbanized sources.

Figure 16: Annual trends in chlorophyll-a and suspended matter concentrations at virtual gauge location 2

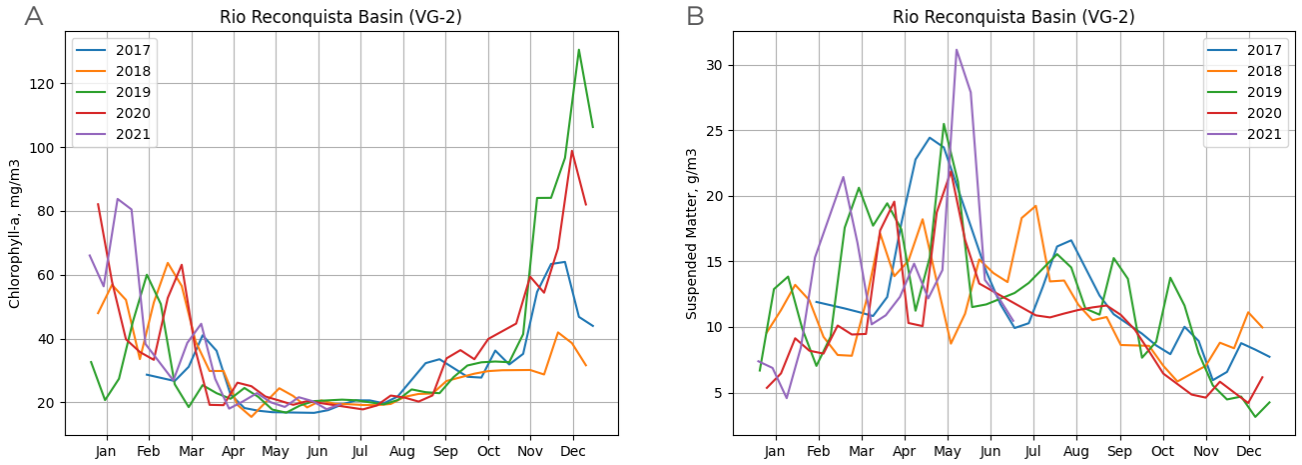

Higher levels of chlorophyll-a (Panel A) from November to March appear to correspond with higher austral summer temperatures. Meanwhile, higher suspended matter concentrations (Panel B) are observed into the wetter months of February to April.

Significant differences were found in WQ metrics observed from Covid-19 lockdown measures at several virtual gauge locations in the Reconquista River Basin (Table 3). Primary lockdown measures in the Buenos Aires region were in effect between March-July 2020, with the full extent summarized in Appendix 1. Of note are the increased chlorophyll-a concentrations at virtual gauges 1, 2, and 3 during Dec/Jan/Feb 2020-2021 of post Covid-19 lockdown. These differences are also observed in maps illustrating the simple difference in mean values between pre- and post-Covid-19 around the virtual gauge locations (Figure 17). While this could point to greater residential wastewater production during lockdown measures, there have also been increasing chlorophyll-a concentrations at virtual gauge locations 1 and 3 since 2016 (Figure 18).

Table 3: WQ metrics observed from Covid-19 lockdown measures at several virtual gauge locations in the Reconquista River Basin

Virtual Gauge #	WQ Metric	Months	Direction of Change (during the observed months)
1	Chlorophyll-a	Dec/Jan/Feb (2020-2021)	Increase
2	Chlorophyll-a	Dec/Jan/Feb (2020-2021)	Increase
2	Susp. Matter & Turbidity	Dec/Jan/Feb (2020-2021)	Decrease
3	Chlorophyll-a	Dec/Jan/Feb (2020-2021)	Increase
3	Chlorophyll-a	Mar/Apr/May (2020)	Increase
3	Susp. Matter & Turbidity	Dec/Jan/Feb (2020-2021)	Decrease
4	Chlorophyll-a	Sep/Oct/Nov (2020)	Increase
4	Turbidity	Dec/Jan/Feb (2020-2021)	Decrease
4	Turbidity	Jun/Jul/Aug (2020)	Increase
4	Turbidity	Mar/Apr/May (2020)	Increase
5	Chlorophyll-a	Jun/Jul/Aug (2020)	Increase
5	Turbidity	Dec/Jan/Feb (2020-2021)	Decrease
5	Turbidity	Jun/Jul/Aug (2020)	Increase
5	Turbidity	Mar/Apr/May (2020)	Increase

Figure 17: Pixel-wise differences between pre- and post-Covid-19 lockdown measures in suspended matter concentrations at virtual gauge locations 1 (Panel A) and 2 (Panel B) in the Río Reconquista Basin

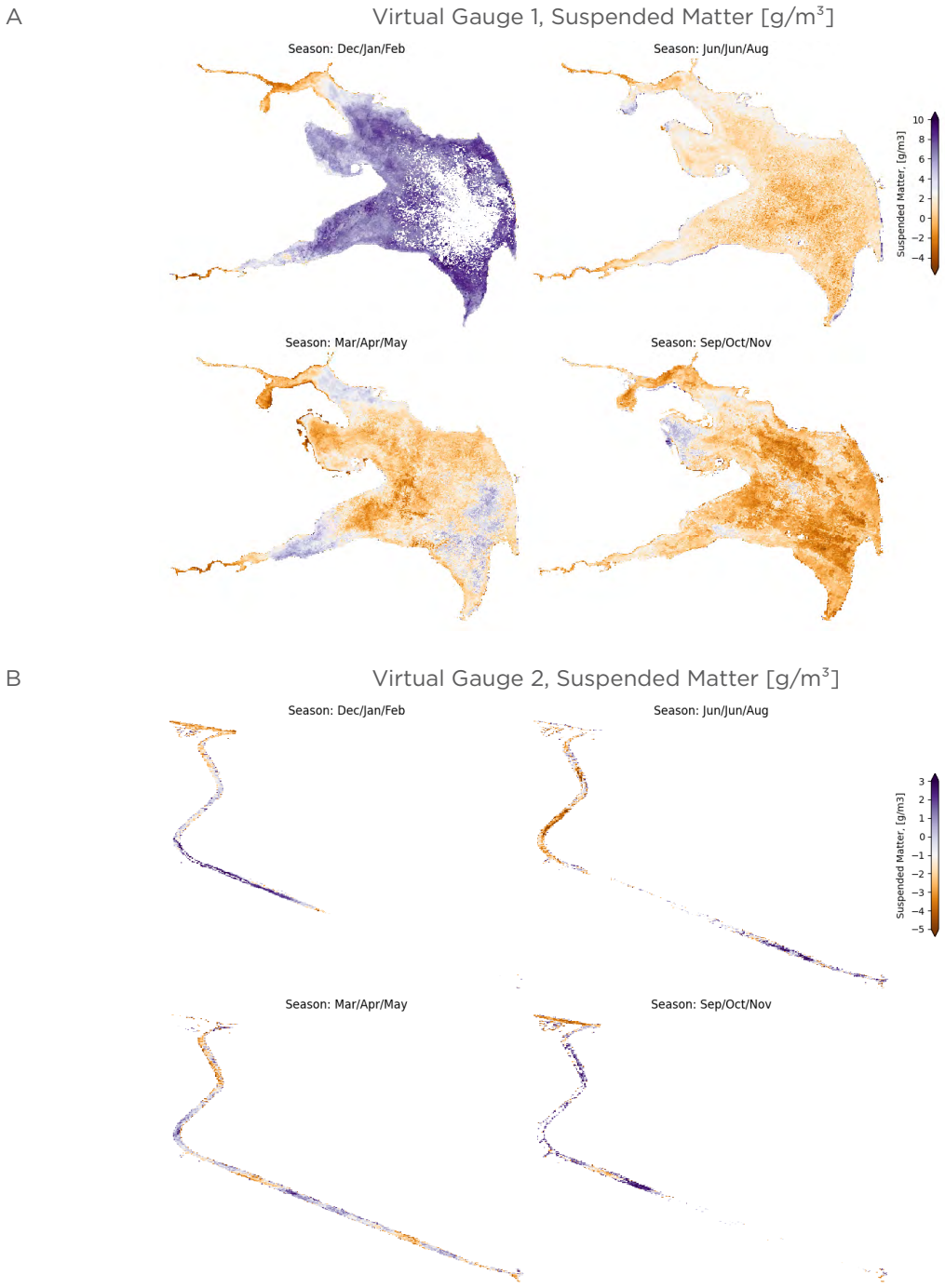

Each 10m pixel depicts the difference in mean WQ metric values between the pre- and post-Covid-19 timeframes. Panel A shows slight increases in suspended matter concentrations in parts of the reservoir from March until November, then a more substantial increase into December and early 2021.

Panel B shows decreased suspended matter concentrations at a few locations throughout virtual gauge location 2 during March/April/May and June/July/August 2020. Of note is the decrease during March/April/May 2020 toward the upstream end of virtual gauge location 2, where the Parque Industrial Tigre is located. Later, in June/July/August 2020, when regional lockdown restrictions began to ease (Appendix 1), the suspended matter concentrations began increasing in this same area.

Figure 18: Long-term trends in chlorophyll-a concentrations at virtual gauges 1 and 3 in Río Reconquista Basin

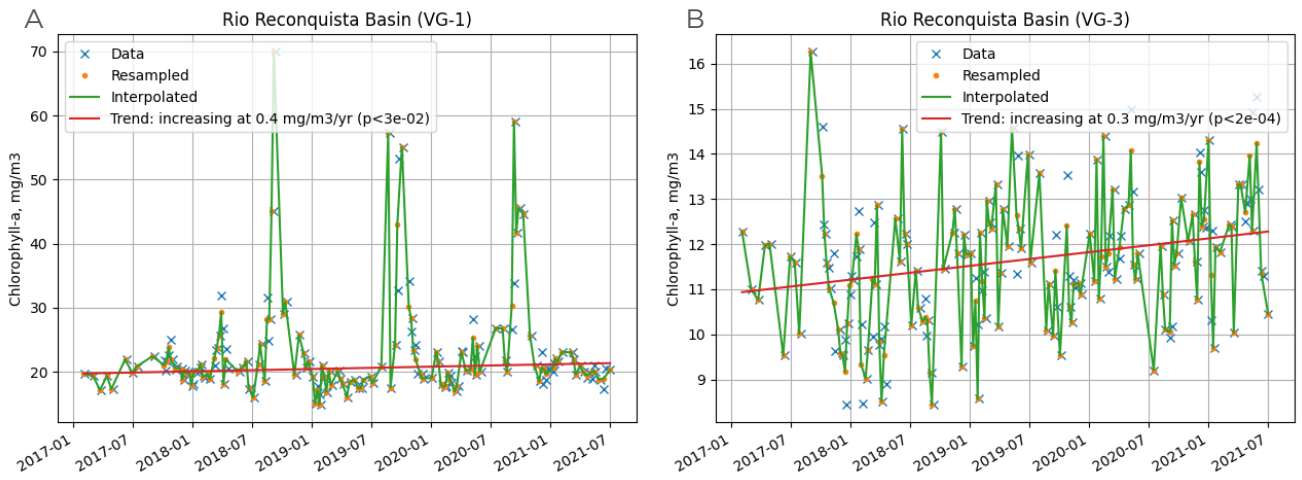

The long-term trends in chlorophyll-a concentrations at virtual gauges 1 and 3 in Río Reconquista Basin show a slight upward trend across the entire time series data set.

These upward trends could be due, in part, to increased runoff of organic compounds from agricultural practices occurring throughout the watershed, which would provide fuel for algae growth.

3.4. Ypacaraí Lake, Paraguay

Located approximately 30 km east of Paraguay's capital city Asunción, Ypacaraí Lake is a major source of drinking and irrigation water for the region, as well as serving as a popular tourist attraction. With a relatively large surface area (60 km^2), average depth of 1.72 m, and location in a subtropical climate, the lake has long suffered from eutrophication and intense algal blooms (Moreira et al., 2018). Additionally, a steadily increasing population with limited access to a formal sewer network results in high organic nutrient loads flowing into the lake. While wetland areas in the north (Yukyry Creek) and south (Pirayú Creek) can filter some of this load, relatively low flow rates from the only outflow point (Salado River) further contribute to algal blooms (Imberger et al., 2017). Consistently high chlorophyll-a concentrations are observed across the entire lake (Figure 19) throughout the entire time series, with notably high values during an algal bloom in March of 2017 (Figure 20). There is a slight seasonal variation in chlorophyll-a concentrations with higher values from June through August (Figure 21), and over the entire time series there is no statistically significant upward or downward trend. Separately, there are significantly increasing trends in suspended matter and turbidity values at all four virtual gauge locations across the lake throughout the entire time series (Figure 22).

Figure 19: Panels A and B show the annual trends in chlorophyll-a and suspended matter concentrations, respectively, across the entire Ypacaraí Lake

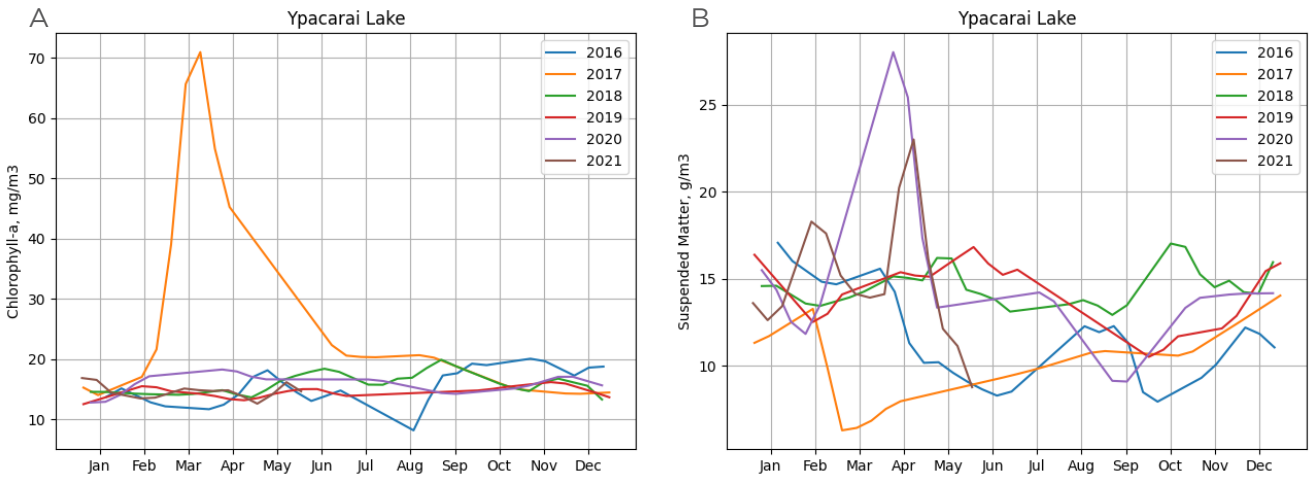

Consistent levels of chlorophyll-a concentrations appear to correspond to the lake's subtropical location, shallow depth, and low turnover rate. A significant spike in chlorophyll-a concentration shows an inverse relationship with suspended matter during an algal bloom in early-mid March 2017. This supports the idea that clear water conditions can predicate intense algae growth and subsequent bloom events.

Figure 20: An intense algal bloom imaged on March 15, 2017

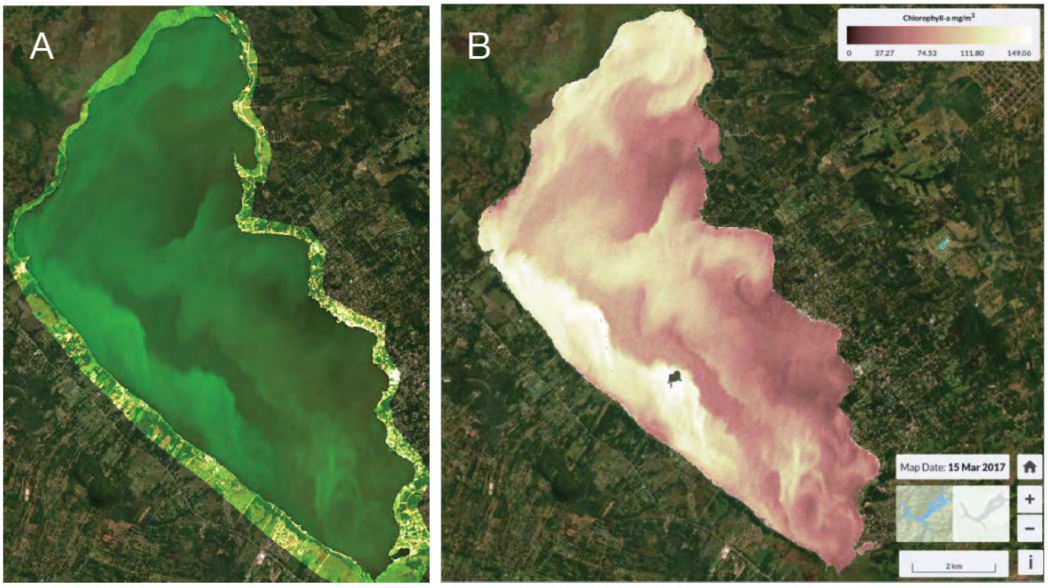

Panel A shows the corrected RGB image, while Panel B shows the calculated chlorophyll-a product. While the average value across the entire reservoir is ~70 mg/m^3, some locations approached 150 mg/m^3. This is a significant deviation from normal values, which ranged from 10-20 mg/m^3 between 2016 and the present. Importantly, this bloom event occurred when lower than normal suspended matter concentrations were observed across the entire reservoir. This demonstrates an inverse relationship between chlorophyll-a and suspended matter concentrations and supports the idea that more clear water allows for increased algae production.

Figure 21: Seasonally partitioned mean chlorophyll-a concentrations across Ypacaraí Lake

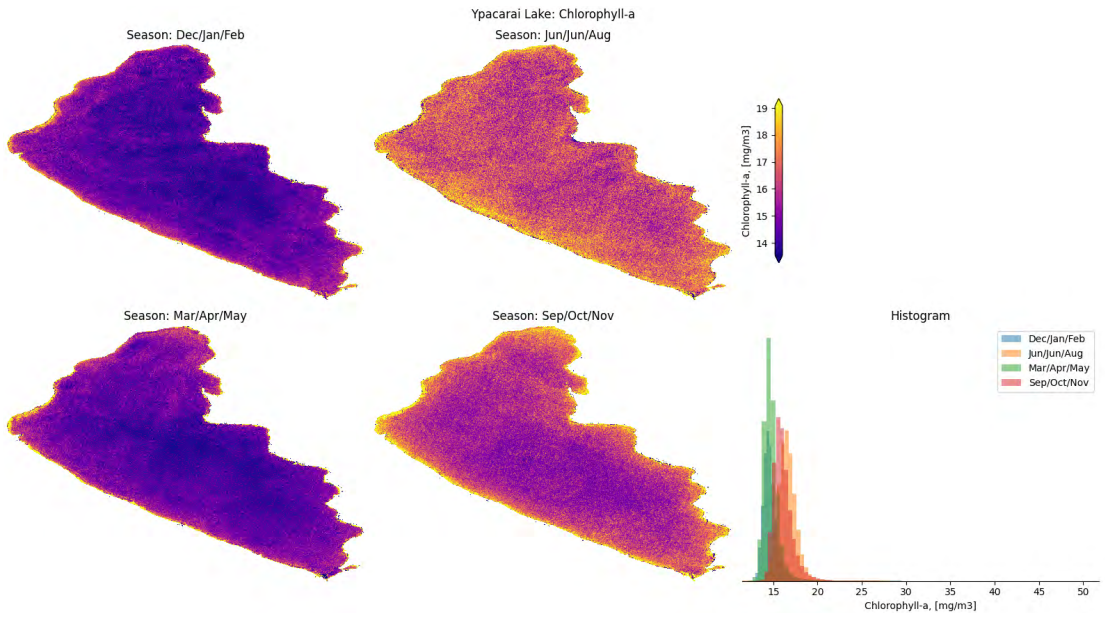

Each surface depicts the mean pixel value across the entire site throughout a three-month period. While there is some localized spatial variation, the small size of this site leads to rather consistent values across the entire area.

Figure 22: Mann-Kendall trend analysis for suspended matter concentrations at all virtual gauge locations at Ypacaraí Lake show an increasing trend since 2016

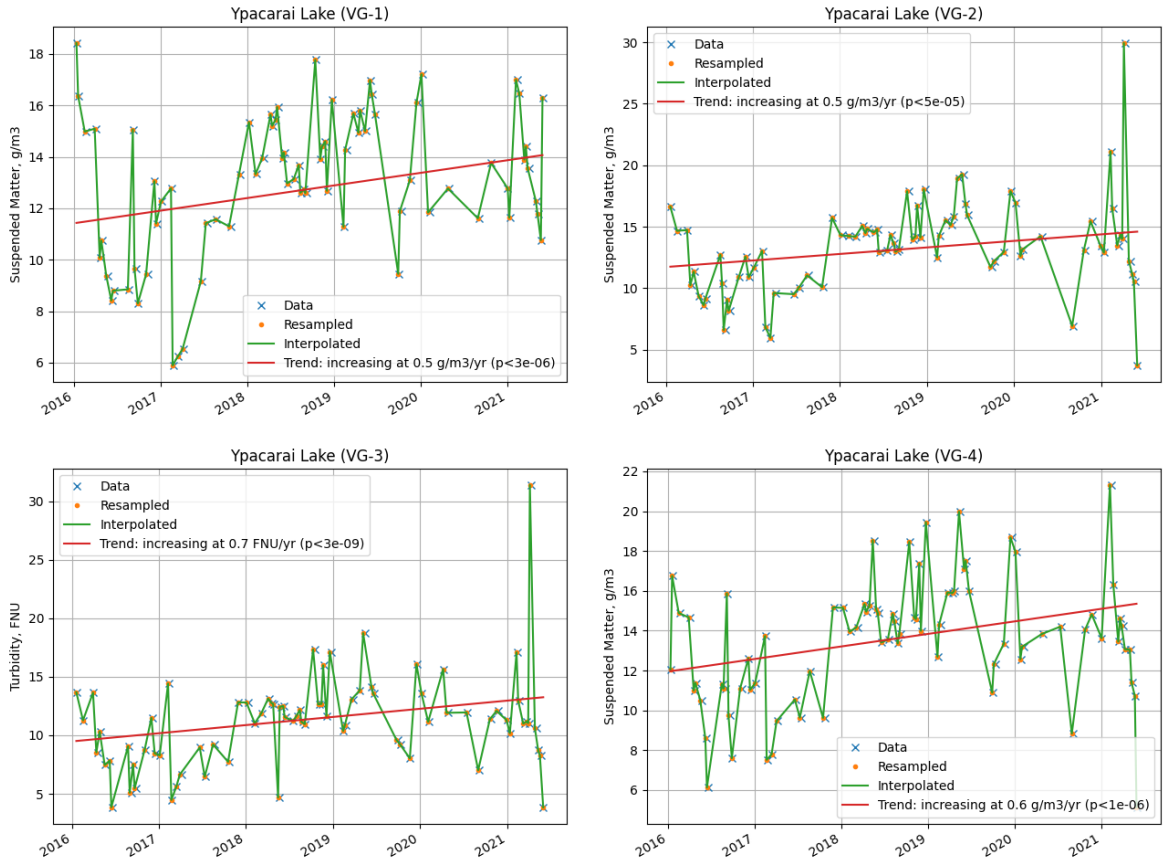

These increasing trends in suspended matter occur while there are no or decreasing trends in chlorophyll-a concentrations at the same virtual gauge locations. Despite the anomalous algal bloom, this could point to how higher overall suspended matter concentrations mitigate algae growth across the entire water body.

No significant differences were found between WQ metrics pre- and post-Covid-19 lockdown measures at any virtual gauge location on Ypacaraí Lake. However, maps illustrating the pixel-wise mean difference between pre- and post-Covid-19 across the entire water surface show observable differences based on season (Figure 23). From March-May of 2020, there is a relatively neutral change signal in chlorophyll-a, while for suspended matter there is an overall decreasing trend. This decreasing trend continues for suspended matter concentrations into June/July/August 2020 before heading in the opposite direction from September 2020 through February 2021. This change in signal could be attributed to limited human activity during the initial lockdown restrictions, then increased travel to the region as people began to work remotely and vacation in the region.

Figure 23: Pixel-wise differences between pre- and post Covid-19 lockdown measures in Chlorophyll-a (Panel A) and suspended matter (Panel B) concentrations across Ypacarai Lake

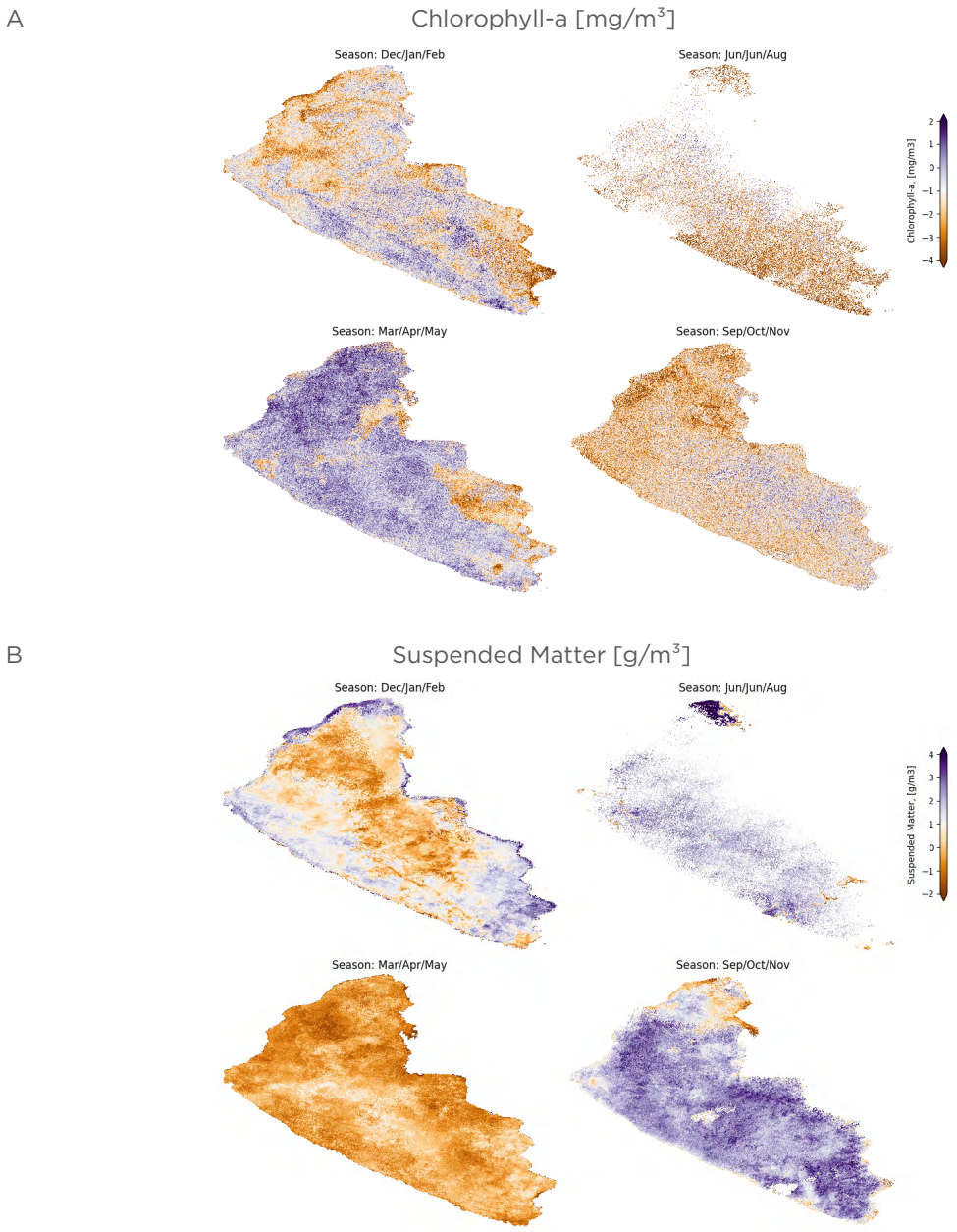

Each 10m pixel depicts the difference in mean WQ metric values between the pre- and post-Covid-19 timeframes. Negative pixel values are areas where there was a significant reduction in a WQ metric when comparing pre- vs. post-Covid-19 lockdown restrictions. Panel B shows that when comparing the months of June/July/August, suspended matter concentrations decreased significantly across the entire water body. This trend then reversed course and increased into the months of September/October/November before becoming more mixed in the months of December/January/February 2020-2021. While these maps likely reflect some of the regular seasonal signal, the significant differences between pre- and post-lockdown conditions should be further investigated.

3.5. Covid-19 Findings

Results of this study show that remote sensing can be used to detect minor and more significant changes in water clarity (turbidity), sediment transport (total suspended matter), and algae (chlorophyll-*a*) concentrations at specific locations during the period coinciding with the Covid-19 lockdown. The timing and duration of lockdown measures vary based on location: Buenos Aires, Argentina from early March to late July 2020; Asunción, Paraguay from early March to late May 2020; La Paz/El Alto, Bolivia from early April to late May; and Río de Janeiro, Brazil during May 2020. These changes were statistically significant in many locations, relative to baseline years prior to 2019. Additionally, the difference maps showed where the most pronounced changes occurred across each site and some of the areas were significant in extent. It is important to note that across all four sites in this pilot, there are no consistent trends in magnitude, spatial extent, or direction of changes. This is likely explained by the diversity of the four water systems in this pilot and the complexity of local land use, mix of runoff (urban and agricultural and intertidal), as well as the prevailing or seasonal hydrological and meteorological conditions.

The most significant changes observed in relation to Covid-19 restrictions generally occurred in areas directly adjoining or downstream from densely populated areas. In the case of Guanabara Bay, significant differences in water quality were observed at several locations in Guanabara Bay (Rio de Janeiro), corresponding to a timeframe that generally coincided with Covid-19 lockdown measures. Chlorophyll-a concentrations have largely decreased across much of Guanabara Bay following COVID-19 lockdown. Chlorophyll-a concentrations at virtual gauge 1, which is near the heavily polluted Río Iguazú's mouth, may have decreased due to shifts in industrial and residential discharges throughout various lockdown stages. However, the rise in chlorophyll-a levels at virtual gauge position 4 during the active lockdown period may be related to an increase in domestic effluent from individuals staying home.

No significant effects on WQ metrics were observed in La Paz/El Alto despite active lockdown measures during April-May 2020 (Appendix 3). The isolated areas downstream from bigger population centers in La Paz, Achacachi, Desaguadero, and Puno, however, showed significant variances at the nearby virtual gauge locations (3 and 5, respectively). These variations could be explained by conducting additional research on local ramifications of lockdown procedures in terms of population migration and effects on water consumption and use of sanitation facilities.

The Reconquista River Basin, which includes the municipality of Buenos Aires, also highlights locations where changes in water quality appear significant and correlated to the timing of Covid-19 restrictions. Primary lockdown measures in the Buenos Aires region between March and July 2020 appear to precede increased chlorophyll-a concentrations across several analysis locations during December 2020 and January/February 2021, which could be indicative of higher untreated or partially treated wastewater production during the lockdown period. It is also important to note that since 2016 -- the start of the Sentinel 2 archive -- there is an underlying trend of increasing eutrophication (as observed from increasing chlorophyll-a concentrations) at specific locations selected in this study (virtual gauges 1 and 3).

There were no statistically significant changes observed in water quality parameters pre- and post-Covid-19 lockdown measures at any study locations on Ypacaraí Lake. However, seasonal differences and long-term increasing trends for suspended sediments across all locations of interest in this pilot are quite notable. Increased sediments could be indicative of long-term increase in nutrient loading from agriculture, which could be driving further eutrophication of this lake. With limited urban development and a population of approximately 350,000 surrounding this water body, the impact of Covid-19 restrictions appears to be minimal.

Generally, the statistically significant changes described above, coinciding with the onset of Covid-19 and the characteristic of being in the vicinity of urban areas, are not generally observed farther downstream or off-shore, as waters get mixed and diluted. This further indicates that observed changes are likely caused by the implemented Covid-19 measures and human-induced changes in urban (residential and industrial) and rural (agricultural) demands on water and sanitation systems. To isolate more localized changes, the remote-sensing data generated from this pilot should be integrated with additional local contexts and datasets describing the extent, timing, and type of impacts observed with regards to water and sanitation locally. Additionally, higher spatial and temporal resolution satellite datasets and local sampling data could be used to build on this local context to provide a highly local or personalized look into human influence changes and trends in water quality at specific locations.

4

CONCLUSIONS

Río Reconquista Basin

4. Conclusions

Remote sensing applied to water quality monitoring in lakes, rivers, and reservoirs is a valuable emerging technology that can provide geospatial information about water clarity and nutrient, bacterial, and industrial pollution from urban and rural sources. The cloud-computing reliant methodology presented in this paper allows rapid monitoring deployment and scalable coverage across numerous watersheds and geographies.

This approach significantly lowers costs of obtaining water quality information compared to laborious water sampling and collection methods. Furthermore, satellite data acquisition and processing are automated and available continuously across the globe, and new data are automatically analyzed and contextualized within seasonal or historical trends. This allows investments in water and sanitation infrastructure to be valued based on realized regional and community benefits and allows water systems operators to reduce risks and lower operational and management costs.

Although this paper presents a comprehensive analysis of this entirely new source of water quality data across the sites and locations of interest, a more detailed analysis can be performed by looking at different timeframes (e.g., entire data set or monthly aggregates) within these watersheds. Additional insights may be revealed by further combining the water quality data sets of this work with other sources of information, including local sensors, information from water and sanitation utilities, and a more detailed analysis of the timing of location conditions and their local impacts.

There is substantive growth in available low-earth orbit satellite imagery or aerial imagery platforms used for observation from private companies such as Planet Labs and public agencies such as NASA, ESA, and others. Significant improvements are expected in the frequency of new image generation. Daily revisits for larger > 5~10 km water areas are already possible. Satellite imagery from commercial platforms is available at 1-meter spatial resolution, enabling access to narrower rivers (>10~20-meter width) and smaller ponds and lakes. These can be easily integrated for specific applications where daily data or high-resolution products are needed. Additionally, autonomous optical sensors provide continuous coverage for smaller streams, and important surface water locations, improving accuracy of data obtained from satellite imagery and providing continuous information when satellite imagery is not available.

These results and remote-sensing technology in general can be a useful addition to the toolkit used by infrastructure and water and sanitation teams in general or more specifically to understand the impacts due to Covid-19 restrictions. The new datasets generated through this pilot can provide insight in three key areas:

a) Inputs on where to measure and optimal in situ sampling rates: Remote sensing results pinpoint locations of high activity and variability throughout the year, optimizing the effectiveness of on the ground sampling by ensuring sampling is happening in the most interesting places.

b) Where to plan and develop future remediation or investment efforts: These data can also be used to identify locations where problems are occurring most frequently, as well as to understand the mitigation or remediation measures that should be applied. In addition to location, the scale of the needed intervention can be determined based on modeled or predicted impacts, and then verified during project implementation.

c) Inputs to help understand the ecological impact of construction, civil engineering, or other infrastructure projects: This remote sensing dataset on water quality gives us insight on what seasonal fluctuations are to be expected, and how levels of different water quality parameters are shifting over the long-term. By combining this dataset with the timing and location of engineering projects or interventions, meteorological and specifically rainfall data, and land use change information more generally, we can reach a more complete understanding of downstream water quality and other environmental impacts from various projects.

This analysis of water quality data sets can be extended by integrating local in situ water quality data, or additional data on meteorological and hydrodynamics, as well as quantified geospatial datasets describing specific changes resulting from socioeconomic conditions (e.g., land use changes) across locations, or other data sets as they become available. Local water quality in situ data would allow validation and calibration of satellite-based retrievals to acquire more quantitative results and the meteorological and hydrological data sets could provide additional context about relationships between water quantity and quality. Additionally, geospatial information about wastewater infrastructure quality, waste outflow locations, and changes in population movement during lockdown could be used to identify locations for study further upstream within the urban system before significant mixing or dilution occurs. These additional datasets and analyses would allow these findings to be applied toward more quantitative and finer resolution scales in time and space.

References

Carreira, R.S., Wagener, A.L.R., Readman, J.W., Fileman, T.W., Macko, S.A., & Álvaro, V. (2002). Changes in the sedimentary organic carbon pool of a fertilized tropical estuary, Guanabara Bay, Brazil: An elemental, isotopic and molecular marker approach. *Marine Chemistry, 79*, 207–227.

Castañé, P. M., Rovedatti, M.G., Topalián, M.L., & Salibían, A. (2006). Spatial and temporal trends of physicochemical parameters in the water of the Reconquista River (Buenos Aires, Argentina). *Environmental Monitoring and Assessment, 117* (1–3), 135–144.

Crúz, M., Terrazas, E.M., & Northcote, T. (2010). Worsening water quality conditions at Inner Puno Bay, Lake Titicaca, Peru, and their effect on Lemna spp. biomass. *Freshwater Forum, 26*(1), 46–57.

Duquesne, F., Vallaeys, V., Vidaurre, P. J., & Hanert, E. (2021). A coupled ecohydrodynamic model to predict algal blooms in Lake Titicaca. *Ecological Modelling, 440*(15), https://doi.org/10.1016/j.ecolmodel.2020.109418.

Fistarol G.O., Coutinho F.H., Moreira, A.P., Venas, T., Cánovas, A., de Paula Jr., S.E., Coutinho R., de Moura, R.L., Valentin, J.L., Tenenbaum, D.R., Paranhos, R., do Valle, R. de A., Vicente, A.C., Amado Filho, G.M., Crespo Pereira, R., Kruger, R., Rezende, C.E., Thompson, C.C., Salomon, P.S., & Thompson, F.L. Environmental and sanitary conditions of Guanabara Bay, Río de Janeiro. (2015). *Frontiers in Microbiology, 6*, 1232. https://doi.org/10.3389/fmicb.2015.01232.

Hirsch, R.M., Slack, J.R., Smith, R.A. (1982). Techniques of trend analysis for monthly water quality data. *Water Resources Research 18*(1): 107-121.

Imberger, J., Marti, C.L., Dallimore, C., Hamilton, D.P., Escriba, J., & Valerio, G. (2017). Real-time, adaptive, self-learning management of lakes. Conference paper presented at the 37th IAHR World Congress. Accessed at https://www.iahr.org/library/infor?pid=2460.

Janches, F., Henderson, H., & MacColman, L. (2014). *Urban Risk and Climate Change Adaptation in the Reconquista River Basin of Argentina*. Lincoln Institute of Land Policy Working Paper. Accessed at https://www.jstor.org/stable/pdf/resrep18470.1.pdf.

Kjerfve, B., Ribeiro, C.H.A., Dias, G.T.M., Filippo, A.M., & da Silva Quaresma, V. (1997). Oceanographic characteristics of an impacted coastal bay: Baía de Guanabara, Río de Janeiro, Brazil. *Continental Shelf Research, 17*(13), 1609–1643.

Mishra, S., & Mishra, D.R. (2012). Normalized difference chlorophyll index: A novel model for remote estimation of chlorophyll-a concentration in turbid productive waters. *Remote Sensing of Environment 117*(3): 394- 406.

Moreira, M.G., Hinegk, L., Salvadore, A., Zolezzi, G., Hölker, F., Domecq, S.R., Bocci, M., Carrer, S., De Nat, L., Escribá, J., Escribá, C., Benítez, G.A., Ávalos, C.R., Peralta, I., Insaurralde, M., Mereles, F., Sekatcheff, J.M., Wehrle, A., Facetti-Masulli, J.F., Toffolon, M. (2018). Eutrophication, research and management history of the shallow Ypacaraí Lake (Paraguay). *Sustainability 10*(7), 2426; https://doi.org/10.3390/su10072426.

Nechad, B., Ruddick, K.G., & Park, Y. (2010). Calibration and validation of a generic multisensor algorithm for mapping of total suspended matter in turbid waters. *Remote Sensing of Environment 114*(4): 854-866.

Appendixes: COVID-19 Lockdown Information

Appendix 1

Buenos Aires, Argentina
Mandatory quarantine (Buenos Aires):
17/03/2020 - 07/11/2020

A brief quarantine to stop the second wave of coronavirus (Buenos Aires):
22/03/2021-31/03/2021

Brief quarantine in 2021: 05/22/2021. People must remain in their habitual residences and may only travel to stock up on cleaning supplies, medicines and food and other necessities in essential businesses. In-person attendance is suspended in economic, industrial, commercial, service, cultural, sports, religious, educational, tourist, recreational and social activities. These measures were applied from Saturday, May 22 at 0:00 until Sunday, May 30, inclusive. As of that day and until June 11, the measures in force continued until May 21, resuming the aforementioned restrictions on the weekend corresponding to June 5 and 6.

Source: Central Government website - medidas gobierno
https://www.argentina.gob.ar/coronavirus/medidas-gobierno

Appendix 2

Asunción, Paraguay
Complete quarantine, officially named “General Preventive Isolation”:
20/03/2020 - 03/05/2020

Smart Quarantine*, Asunción (*Cuarentena inteligente):
04/05/2020 - 24/05/2020 (Phase 1)
25/05/2020 - 14/06/2020 (Phase 2)
15/06/2020 -22/08/2020 (Phase 3)

Social Quarantine*, Asunción (*Cuarentena social):
23/08/2020 - 04/10/2020

New Normal* (*Nueva Normalidad):
05/10/2020 – until now

Red Zones, Asunción (*Zonas rojas):
18/03/2021 - 26/03/2021
27/04/2021 - 10/05/2021

Total quarantine:
Paraguay (including Asunción) entered a total quarantine on March 20, 2020, when community transmission was confirmed in the country, totally restricting free movement, except in cases of necessity or urgency, and certain workers were exempted, especially in basic services (supermarkets, pharmacies, service stations, among others). Curfew: 24 hours.

Smart Quarantine (Cuarantena inteligente)
The 'Smart Quarantine', officially called the 'Plan for the Gradual Lifting of General Preventive Isolation', consists of the release of certain labor sectors (and in phases) for the gradual and monitored activation of the economy, under strict sanitary measures that were presented on April 24 and in force since May 4. It is made up of four phases, in which the epidemiological situation and civic behavior are analyzed every 21 days to gradually release the other phases. (Phase 1: preparation, Phase 2: mild, Phase 3: moderate). Curfew: 9:00 p.m. to 5:00 a.m. (Phases 1,2) / 11:00 p.m. to 5:00 a.m. (Sunday to Thursday) 12:00 a.m. to 5:00 a.m. (Friday and Saturday) (Phase 3)

Social quarantine (Cuarentena social)
On August 20, 2020, the Minister of Health announced that from Monday, August 24 to Sunday, September 6, new restrictions would be in force, especially for the social sphere, called "Social Quarantine", to be applied in Asunción and the Central department for 15 days. On September 4, it was extended until September 20. On September 18, it was extended until October 4. Curfew: 20:00 to 05:00.

New Normal
As announced on October 2, 2020, by the Minister of Health, the Quarantine phases were lifted throughout the country, to move toward a new normality known as the "covid way of living", releasing most of the activities but maintaining health care. Curfew: 00:00 to 05:00.

Red Zones (Zonas rojas)
From March 18 to March 26, 2021, the Ministry of Public Health and Social Welfare designated districts, including Asunción, as "red zones". From April 27 to May 10, 2021, the government once again established new measures in the red zones, including Asunción. Curfew: 20:00 to 05:00.

Source: Ministry of Public Health and Social Wellbeing (MINISTERIO de SALUD PÚBLICA y BIENESTAR SOCIAL)
https://www.mspbs.gov.py/dependencias/portal/adjunto/36a471-DecretoN3478MedidasSanitarias.pdf
https://dgvs.mspbs.gov.py/

Appendix 3

La Paz/El Alto, Bolivia
Full quarantine:
04/29/2020 - 05/31/2020* (not as strict as other countries or Oruro and Santa Cruz)

Dynamic quarantine* (*Cuarentena dinámica):
06/01/2020 - 08/31/2020
*07/16/2020 - 07/19/2020 (rigid quarantine)

Post quarantine:
09/01/2020 – now

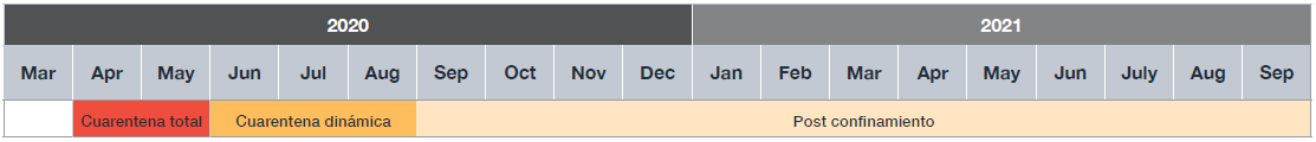

Dynamic quarantine in La Paz: The Municipal Law established a series of measures that must be applied to prevent the spread and community contagion of COVID-19 in the Municipality of La Paz, as the population resumes its activities, with state authorization and under regulation of current regulations. For this purpose, the powers of the Municipal Executive Body of the Autonomous Municipal Government of La Paz were established, to be exercised within the framework of the Conditional Dynamic Quarantine.

Post Confinement: Within the framework of entering the post confinement phase established in Supreme Decree No. 4314, measures were provided to be implemented as of September 1, 2020 in the Municipality of La Paz, in accordance with the provisions). The following articles of this decree: The hours allowed for pedestrian circulation extend from 05:00 to 20:00 from Monday to Friday.

*Although the second wave hit hard in La Paz around Nov.-Dec. 2020, they did not decree a quarantine.

Source: Observatorio Covid 19 - La Paz gobierno
http://observatoriocovid19.lapaz.bo/observatorio/index.php/component/phocadownload/category/11-politico

Appendix 4

Río de Janeiro, Brazil
2020 Lockdown in Río:
10/05/2020 - 24/05/2020

2021 Lockdown in Río:
20/03/2021 - 04/04/2021

2020										2021								
Mar	Apr	May	Jun	Jul	Aug	Sep	Oct	Nov	Dec	Jan	Feb	Mar	Apr	May	Jun	July	Aug	Sep
		Lock-down										Lock-down						

2020: In Río de Janeiro, the lockdown was adopted in the municipality of Niterói, by decree of Mayor Rodrigo Neves, scheduled to start after Mother's Day (May 10). Only health and safety professionals were allowed to leave their home, except in urgent cases for ordinary citizens. The lockdown started on May 18th and ended on the 24th.

2021: On March 19, the Municipality of Campos dos Goytacazes, in Norte Fluminense, announced the closure of the city's shops, which began the following day. The published document restricted the operation of bars, kiosks, beverage deposits, restaurants, snack bars, pizzerias and the like until April 4.

Sources
https://pt.wikipedia.org/wiki/Lockdown_no_Brasil_em_2020
https://pt.wikipedia.org/wiki/Lockdown_no_Brasil_em_2021


IDB